Zoological Journal of the Linnean Society, 2022, **194**, 181–225. With 25 figures.

Exploring the diversity of the deep sea—four new species of the amphipod genus *Oedicerina* described using morphological and molecular methods

ANNA M. JAŻDŻEWSKA[1,*], ANGELIKA BRANDT[2,3], PEDRO MARTÍNEZ ARBIZU[4] and ANNEMIEK VINK[5]

[1]*Department of Invertebrate Zoology and Hydrobiology, Faculty of Biology and Environmental Protection, University of Lodz, Lodz, Poland*
[2]*Senckenberg Research Institute and Natural History Museum, Frankfurt am Main, Germany*
[3]*Institute for Ecology, Evolution and Diversity, Goethe-University of Frankfurt, Frankfurt am Main, Germany*
[4]*German Center for Marine Biodiversity Research (DZMB), Senckenberg am Meer, Südstrand 44, D-26382 Wilhelmshaven, Germany*
[5]*Marine Geology, Federal Institute for Geosciences and Natural Resources, 30655, Hannover, Germany*

Received 4 August 2020; revised 25 March 2021; accepted for publication 16 April 2021

Collections of the amphipod genus *Oedicerina* were obtained during six expeditions devoted to the study of deep-sea environments of the Pacific Ocean. The material revealed four species new to science. Two species (***Oedicerina henrici* sp. nov.** and ***Oedicerina teresae* sp. nov.**) were found at abyssal depths of the central eastern Pacific in the Clarion-Clipperton Zone; one species **(*Oedicerina claudei* sp. nov.)** was recovered in the Sea of Okhotsk (north-west Pacific), and one **(*Oedicerina lesci* sp. nov.)** in the abyss adjacent to the Kuril-Kamchatka Trench (KKT). The four new species differ from each other and known species by the shapes of the rostrum, coxae 1 and 4, basis of pereopod 7, armatures of pereonite 7, pleonites and urosomites. An identification key for all known species is provided. The study of the cytochrome *c* oxidase subunit I gene of the four new species and *Oedicerina ingolfi* collected in the North Atlantic confirmed their genetic distinction. However, small intraspecific variation within each of the studied species was observed. In the case of the new species occurring across the KKT, the same haplotype was found on both sides of the trench, providing evidence that the trench does not constitute an insurmountable barrier for population connectivity. None of the species have so far been found on both sides of the Pacific.

ADDITIONAL KEYWORDS: abyssal – Amphipoda – central eastern Pacific – Clarion-Clipperton Zone – *COI* – Crustacea – north-west Pacific – taxonomy.

INTRODUCTION

Deep-sea exploration for mineral resources of the seafloor has increased in the last decade and several research programs have been conducted to study this largest and least-explored ecosystem on Earth. Among the areas that have gained particular scientific and economic interest is the Clarion-Clipperton Zone (CCZ) in the central Pacific due to the presence of polymetallic nodule fields (Glover *et al.*, 2016; Janssen *et al.*, 2019; Christodoulou *et al.*, 2020). Another deep-sea region that was recently extensively sampled covers a large area of the north-west (NW) Pacific, namely the Sea of Japan, the Sea of Okhotsk and the Kuril-Kamchatka Trench (KKT) with the abyssal plain adjacent to it (Malyutina & Brandt, 2013; Brandt & Malyutina, 2015; Malyutina *et al.*, 2018; Brandt *et al.*, 2020). The sampling gear used nowadays

*Corresponding author. E-mail: anna.jazdzewska@biol.uni.lodz.pl
[Version of record, published online 18 June 2021; http://zoobank.org/ urn:lsid:zoobank.org:pub:01794248-7D36-42DC-B1FD-2A61FBEEB577

during scientific cruises, the Brenke-type epibenthic sledge in particular (Brandt & Barthel, 1995; Brenke, 2005), enables the collection of the small-sized fraction of deep-sea fauna that was often neglected during previous expeditions. Moreover, change in practice of sample fixation and subsequent storage provide material available for molecular examination. Such an approach revealed an unexpectedly high diversity of deep-sea fauna including recognition of a number of species new to science, for both macrobenthic (Polychaeta, Ophiuroidea, Isopoda and Amphipoda) and meiobenthic (harpacticoid Copepoda) groups (Glover *et al.*, 2002; Janssen *et al.*, 2015; Jażdżewska & Mamos, 2019; Brix *et al.*, 2020; Christodoulou *et al.*, 2020; Khodami *et al.*, 2020).

Currently, scientists are putting effort into formally describing these new taxa (e.g. Bober *et al.*, 2018b; Bonifácio & Menot, 2019; Renz *et al.*, 2019; Dong *et al.*, 2021; Kaiser *et al.*, 2021). Another example includes 29 species new to science from various taxa described in a single volume of *Progress in Oceanography*, summarizing results from NW Pacific deep-sea exploration (Brandt *et al.*, 2020). However, because describing species is a time-consuming process, many new species remain as morphologically identified Operational Taxonomical Units (OTU) or Molecular Operational Taxonomic Units (MOTU), and only given temporary names or codes. Such an approach allows for preliminary assessment of biodiversity, but it is important to stress that only species with names are recognized by the scientific community and society and only named species can become a subject of conservation (Delić *et al.*, 2017; Britz *et al.*, 2020). Moreover, only the species with described morphology can be compared with historical collections or recent material unavailable for molecular studies (Dupérré, 2020). The description of new species provides a baseline for further ecological or biogeography studies and as such it is a crucial and the only sustainable step in recognition of species and their service for ecosystem functioning.

The Amphipoda belong to the brooding peracarid crustaceans (Malacostraca) and form an abundant component of the deep-sea benthos. As an example, in the NW Pacific, deep-sea Amphipoda may constitute *c*. 7% of the total faunal abundance and are outnumbered by the Annelida, Copepoda and Isopoda. Similar values of abundance in that area were recorded for the Bivalvia and Ophiuroidea (Brandt *et al.*, 2019). Within peracarids, deep-sea Amphipoda and Isopoda are the two dominant orders jointly constituting from 50% to almost 90% of the abundance and 60–80% of recognized species (Frutos *et al.*, 2017; Brandt *et al.*, 2019). However, amphipod diversity and abundance is known to be high in the bathyal (40–60% of species, 25–50% of abundance) and usually decreases towards abyssal and hadal depths (Frutos *et al.*, 2017; Brandt *et al.*, 2019). In the South Polar Front, deep-sea Amphipoda are less abundant than Isopoda and probably also less species rich (Brandt *et al.*, 2014). More than 400 species of deep-sea benthic amphipods (recorded below 2000 m) are currently known, but it does not reflect the actual deep-sea amphipod species richness. For example, from only three deep-sea Antarctic expeditions, approximately 500 species new to science still await to be described (Jażdżewska, 2015).

The family Oedicerotidae is represented by 47 known genera and 246 species (Horton *et al.*, 2020). This diverse family, including primarily infaunal species, constitutes an abundant component of benthic amphipod communities at all latitudes and depths (Weisshappel & Svavarsson, 1998; Jażdżewska, 2015; Brix *et al.*, 2018b; Vause *et al.*, 2019). Among oedicerotid genera, *Oedicerina* Stephensen, 1931 appears to be a typical deep-sea taxon. Its shallowest known record comes from a trawl conducted between 200 and 500 m in depth (Ledoyer, 1986), while all other records are between 470 m (Coleman & Thurston, 2014) and 4050 m (Hendrycks & Conlan, 2003). Five species are described in *Oedicerina* to date: *Oedicerina ingolfi* Stephensen, 1931, *Oedicerina megalopoda* Ledoyer, 1986, *Oedicerina denticulata* Hendrycks & Conlan, 2003, *Oedicerina loerzae* Coleman & Thurston, 2014 and *Oedicerina vaderi* Coleman & Thurston, 2014.

The study of the material of *Oedicerina* obtained during six deep-sea expeditions to the central east and NW Pacific revealed four species new to science that are described here in detail. Additionally, an analysis of the mitochondrial cytochrome *c* oxidase subunit I gene (*COI*) was conducted in order to provide barcodes for the new species that together with scientific descriptions will be useful to unravel the ranges of species distributions and their biogeography in the abyss.

MATERIAL AND METHODS

The material examined consisted of 37 individuals sampled during six deep-sea expeditions (Table 1). Of these, seven individuals were collected from the central east Pacific (CCZ) and an additional 30 specimens from the NW Pacific.

The Clarion-Clipperton Zone (CCZ)

The CCZ is regarded as the area between the Clarion and Clipperton Fracture Zones in the central east Pacific and it is characterized by the presence of

Table 1. Stations sampled during six scientific cruises during which new *Oedicerina* species were found. CCZ = Clarion Clipperton Zone, UKSR area = United Kingdom (UK Seabed Resources Ltd.) exploration zone, BGR area = German (Bundesanstalt für Geowissenschaften und Rohstoffe) exploration zone, KKT = Kuril-Kamchatka Trench

Station code	Latitude	Longitude	Depth (m)	Date	No of ind.	Region	Sector
ABYSSLINE-2							
AB2-EB04	12°07.83' N-12°08.02' N	117°18.67' W-117°17.52' W	4111–4122	25 Feb 2015	1	CCZ	UKSR area
AB2-EB12	12°02.72' N-12°03.03' N	117°25.43' W-117°24.28' W	4223–4299	16 Mar 2015	1	CCZ	UKSR area
MANGAN 2016							
Ma-16-25	11°49.143' N-11°49.975' N	116°58.492' W-116°57.797' W	4107–4101	24 Apr 2016	1	CCZ	BGR area
Ma-16-28	11°49.654' N-11°49.902' N	117°00.299' W-116°59.174' W	4143–4133	1 May 2016	1	CCZ	BGR area
Ma-16-95	11°47.862' N-11°47.152' N	117°30.639' W-117°29.490' W	4356–4359	9 May 2016	2	CCZ	BGR area
MANGAN 2018							
SO-262-156	11°49.381' N-11°49.752' N	117°32.663' W-117°30.760' W	4340–4340	9 May 2018	1	CCZ	BGR area
KuramBio I							
SO-223-1-11	43°58.44' N-43°58.61' N	157°18.29' E-157°18.13' E	5418–5419	30 Jul 2012	1	NW Pacific	Abyssal plain of the KKT
SO-223-2-9	46°14.78' N-46°14.92' N	155°32.63' E-155°32.57' E	4830–4863	3 Aug 2012	1	NW Pacific	Abyssal plain of the KKT
SO-223-3-9	47°14.66' N- 47°14.76' N	154°42.88' E-154°43.03' E	4987–4991	5 Aug 2012	19	NW Pacific	Abyssal plain of the KKT
SO-223-9-9	40°34.51' N- 40°34.25' N	150°59.92' E-150°59.91' E	5399–5421	23 Aug 2012	1	NW Pacific	Abyssal plain of the KKT
SO-223-10-9	41°12.80' N- 41°13.01' N	150°06.162' E-150°05.652' E	5245–5262	26 Aug 2012	1	NW Pacific	Abyssal plain of the KKT
KuramBio II							
SO-250-85	45°02.26' N-45°01.64' N	151°02.14' E-151°03.68' E	4903–5266	15 Sep 2016	1	NW Pacific	Abyssal plain of the KKT
SokhoBio							
AKL-71-1-9	46°05.037' N- 46°08.727' N	146°00.465' E-146°00.227' E	3307–3307	10 Jul 2015	1	NW Pacific	Sea of Okhotsk
AKL-71-10-5	46°07.410' N-46°07.310' N	152°11.292' E-152°11.537' E	4681–4702	28 Jul 2015	1	NW Pacific	Abyssal plain of the KKT
AKL-71-10-7	46°06.027' N-46°05.827' N	152°14.439' E-152°14.576' E	4769–4798	29 Jul 2015	4	NW Pacific	Abyssal plain of the KKT

polymetallic nodule fields (Wiklund *et al.*, 2019). In total, the area covers approximately 6 million km^2; however, in the present study only the easternmost sector of the zone was considered. The material collected in the CCZ came from three scientific expeditions. The ABYSSLINE-2 (ABYSSal baseLINE project) expedition, on board the R/V *Thomas F. Thompson*, was conducted in 2015 and collected samples from the UKSR License Area (UK Seabed Resources Ltd, United Kingdom). The other two expeditions, MANGAN 2016 and MANGAN 2018, sampled the German License Area (BGR—Bundesanstalt für Geowissenschaften und Rohstoffe) on board the R/V *Kilo Moana* and R/V *Sonne*, respectively.

The north-west Pacific study area (NW Pacific)

The area around the Sea of Okhotsk was surveyed during the SokhoBio expedition in 2015 using the R/V *Akademik Lavrentyev* (Malyutina *et al.*, 2018). The KKT and its adjacent abyssal plain was explored with the R/V *Sonne* in 2012 and 2016 during the KuramBio I and II expeditions, respectively (Brandt *et al.*, 2020). Details of the oceanographic features of the studied area are available in Malyutina & Brandt (2013), Brandt & Malyutina (2015), Saeedi & Brandt (2020), and Brandt *et al.* (2020).

Sample collection and processing

The samples used in this study were collected using two types of epibenthic sleds: a Brenke-type sled (Brandt & Barthel, 1995; Brenke, 2005) and a camera-equipped epibenthic sled [C-EBS (Brandt *et al.*, 2013)]. The deployment protocol followed Brenke (2005). Upon recovery, samples were passed through 300 μm and either sorted out immediately and preserved in 80% ethanol kept at -20 °C, or immediately transferred into chilled (-20 °C) 96% ethanol. In the second case, the sorting by stereomicroscope was carried out after 48 h storage in a -20 °C freezer (Riehl *et al.*, 2014).

Morphological study

Individuals were initially examined using either a Leica M125 (CCZ material) or a Nikon SMZ800 (NW Pacific material) stereomicroscope. Hand drawings of the habitus of the species identified in the Sea of Okhotsk and KKT area were prepared using a Nikon SMZ1500 stereomicroscope equipped with a camera lucida. The habitus of the species from the central Pacific are presented as photographs obtained with a confocal laser scanning microscope (CLSM). The holotypes were stained in Congo red and acid fuchsin, temporarily mounted onto slides with glycerin and examined with a Leica TCS SPV equipped with a Leica DM5000 B upright microscope and three visible-light lasers (DPSS 10 mW 561 nm; HeNe 10 mW 633 nm; Ar 100 mW 458, 476, 488 and 514 nm), combined with the software LAS AF 2.2.1 (Leica Application Suite, Advanced Fluorescence). A series of photographic stacks were obtained, collecting overlapping optical sections throughout the whole preparation (Michels & Büntzow, 2010; Kamanli *et al.*, 2017). All individuals, except for those whose posterior part of the body was broken, were measured (from the tip of the rostrum to the end of the telson) and chosen specimens were dissected and mounted on permanent slides using polyvinyl-lactophenol containing lignin pink. All slides were examined using a Nikon Eclipse Ci compound microscope equipped with a camera lucida. Pencil drawings from the microscope were used as the basis for line drawings. The drawings were inked with Adobe Illustrator CS6 following the recommendations of Coleman (2003, 2009).

The following terminology has been applied concerning setation and extensions of the cuticle (modified from d'Udekem d'Acoz, 2004): tooth—non-articulated extension of the cuticle; seta—articulated slender extension (may be short or long, plumose, serrate, denticulate, cuspidate or smooth); setule—very small and delicate short seta; spine—articulated robust extension (usually short).

In the descriptions and figures the following abbreviations were used: A1, 2 = antenna 1, 2; UL = upper lip; LL = lower lip; Md = mandible; Mx1, 2 = maxilla 1, 2; Mxp = maxilliped; c1–4 = coxa 1–4; G1, 2 = gnathopod 1, 2; P3–7 = pereopod 3–7; pl1–3 = pleopod 1–3; U1–3 = uropod 1–3; T = telson.

Apart from the standard measurements typically used for descriptions of amphipods, two additional ones were provided. One expresses the curvature of the rostrum (the angle between the dorsal margin of the head and the frontal margin of the rostrum—Fig. 1A-B), the second one measures the width to depth ratio of the posterior lobe of coxa 4 (Fig. 1C).

The registered type material is deposited in the Zoological Museum of Hamburg (CeNak), Germany (ZMH), in the Senckenberg Museum (Frankfurt, Germany) (SMF) and in the National Scientific Center of Marine Biology (Vladivostok, Russia) (MIMB). All the remaining material is kept in the scientific collection of the Department of Invertebrate Zoology and Hydrobiology, University of Lodz, Poland. The summary of all studied individuals is provided in the Supporting Information (Table S1).

Molecular investigation

Eighteen individuals representing each identified species (from one to ten individuals per species)

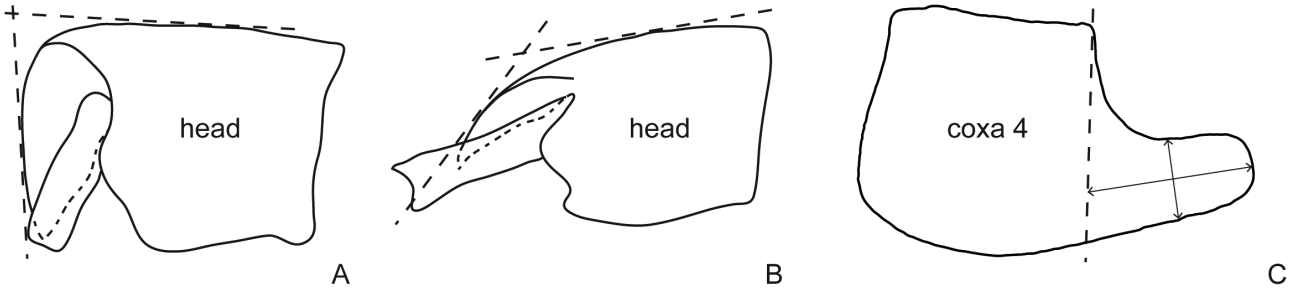

Figure 1. A, B, *Oedicerina* sp. head presenting the curvature of rostrum. Dashed lines show the dorsal margin of the head and front margin of the rostrum. A, rostrum strongly deflexed (the angle between both margins *c.* 90°). B, rostrum curved but not strongly deflexed (wide angle between both margins). C, presentation of the measurement of the width to depth ratio of the posterior lobe of coxa 4. The dashed line indicates how the lobe was defined.

were chosen for cytochrome *c* oxidase subunit I gene (*COI*) analysis. Additionally, five individuals of *O. ingolfi* collected in North Atlantic during the IceAGE 1 and 2 expeditions (Brix *et al.*, 2018b) were used in our molecular study. The total genomic DNA was extracted from one pleopod (if the posterior part of the body was missing the last present leg was used). The DNA extraction of individuals from the Central Pacific and from the North Atlantic was performed using 100 µL InstaGene Matrix (BIO-RAD). Digestion was carried out at 56 °C for 40 min. The extraction of individuals collected from the NW Pacific was carried out using a mixture of 150 µL pure H_2O with 0.015 g Chelex (Sigma-Aldrich Co.) and 10 µL proteinase K. The digestion at 55 °C lasted for 6 h.

The DNA barcoding fragment of *COI* (658 bp) was amplified using the degenerate LCO1490-JJ (CHACWAAYCATAAAGATATYGG) and HCO2198-JJ (AWACTTCVGGRTGVC CAAARAATCA) primer pair (Astrin & Stüben, 2008). In the case of the CCZ and the North Atlantic specimens, polymerase chain reaction was performed with AccuStart II PCR SuperMix (Quantabio), whereas for the NW Pacific specimens DreamTaq Green PCR Mastermix (Thermo Scientific) was used. In both cases the reaction conditions followed Hou *et al.* (2007). Sequences were obtained by Macrogen Inc. (the Netherlands) on an Applied Biosystems 3730xl capillary sequencer. One-way (forward) sequencing was the standard procedure for all samples, but in addition, at least one individual of each species (preferably the holotype) was sequenced in both directions. As a result, each species received at least one sequence of the barcode fragment of the full length. Electropherograms were viewed in Geneious 10.1.2 and primer sequences and ambiguous positions were trimmed. Sequences were initially blasted using default parameters on NCBI BLASTn and translated into amino acid sequences to confirm that no stop codons were present. All sequences were deposited in GenBank with the accession numbers: MN346926 and MW377925-MW377946. Relevant voucher information, taxonomic classifications and sequences are deposited in the data set "DS-OEDICERI" in the Barcode of Life Data System (BOLD) (dx.doi.org/10.5883/DS-OEDICERI) (www.boldsystems.org) (Ratnasingham & Hebert, 2007).

The sequences were subjected to the Barcode Index Number (BIN) System (Ratnasingham & Hebert, 2013) in BOLD. It compares newly submitted sequences with the sequences already available. They are clustered according to their molecular divergence using distance-based algorithms (single linkage clustering followed by Markov clustering) that aim at finding discontinuities between Operational Taxonomic Units (OTU). Each OTU receives a unique and specific code (BIN), either already available or new if submitted sequences do not cluster with already-known BINs.

All sequences were aligned with the MAFFT v.7.308 algorithm (Katoh *et al.*, 2002; Katoh & Standley, 2013) in Geneious 10.1.2, resulting in a 615 bp alignment. The uncorrected *p*-distance and the Kimura 2-parameter (K2P) model (Kimura, 1980) were used to calculate sequence divergence in MEGA v.7.0.18 (Kumar *et al.*, 2016). A Neighbour-Joining (NJ) tree of all sequences was built based on the uncorrected *p*-distance matrix, with both transitions and transversions included and all positions with gaps or missing data removed (Saitou & Nei, 1987). Node support was inferred with a bootstrap analysis (1000 replicates) (Felsenstein, 1985). The *COI* sequence of another oedicerotid, *Arrhis phyllonyx* (M. Sars, 1858) (GenBank accession number MG264772; Jażdżewska *et al.*, 2018), was used as an outgroup. To visualize molecular divergence of *COI* haplotypes (with all ambiguous positions excluded), a Median

Joining Network for each species was generated using PopART 1.7 (Bandelt *et al.*, 1999).

RESULTS

SPECIES DESCRIPTIONS

ORDER AMPHIPODA LATREILLE, 1816

SUBORDER AMPHILOCHIDEA BOECK, 1871

FAMILY OEDICEROTIDAE LILLJEBORG, 1865

GENUS *OEDICERINA* STEPHENSEN, 1931

Known species: Oedicerina ingolfi Stephensen, 1931; *O. megalopoda* Ledoyer, 1986; *O. denticulata* Hendrycks & Conlan, 2003; *O. loerzae* Coleman & Thurston, 2014; *O. vaderi* Coleman & Thurston, 2014.

OEDICERINA HENRICI JAŻDŻEWSKA, **SP. NOV.**

(FIGS 2–6)

Zoobank registration: urn:lsid:zoobank.org:act:9A993D45-B781-4479-A4D6-2EC840D1BC3E.

Type material

Holotype: ♂, 6.5 mm, body remnants and two slides with appendages, ZMH K-60658, DSB_3762, St. AB2-EB04, 12°07.83’ N, 117°18.67’ W-12°08.02’ N, 117°17.52’ W, 4111–4122 m, 25 February 2015, leg. Inga Mohrbeck.

Paratype: Immature ♂, urosome missing, individual originally in one piece, broke into three parts during examination, one slide with appendages, ZMH K-60659, DSB_3682, St. Ma 16–95, 11°47.862’ N, 117°30.639’ W-11°47.152’ N, 117°29.490’ W, 4356–4359 m, 9 May 2016, leg. Annika Janssen.

Additional material: One ovigerous ♀ (single egg), individual found in two parts, DNA is extracted from the anterior part, posterior part preserved but not used for taxonomic evaluation, ZMH K-60660, DSB_3582, St. SO 262-156, 11°49.381’ N, 117°32.663’ W-11°49.752’ N, 117°30.760’ W, 4340–4340 m, 9 May 2018, leg. Pedro Martínez Arbizu.

The registered type material is deposited in the Zoological Museum of Hamburg, Germany.

Type locality: Eastern central Pacific, CCZ, St. AB2-EB04, 12°07.83’ N, 117°18.67’ W-12°08.02’ N, 117°17.52’ W, 4111–4122 m.

Etymology: The species is named for Prof. Krzysztof Henryk (Latin *Henricus*) Jażdżewski, the first author’s father and renowned specialist in amphipod taxonomy, diversity and ecology.

Description: Based on male, 6.1 mm, St. AB2-EB04. *Head* (Fig. 2): longer than deep, longer than pereonites 1–3 combined; no eyes or ocular pigment visible; rostrum strongly deflexed, the angle between head dorsal margin and rostrum margin 90 ° or less, rostrum as long as first article of peduncle of antenna 1; interantennal lobe weak, rounded. *Antenna 1* (Fig. 3; broken in holotype at first peduncular article, description based on paratype): length ratios of peduncle articles 1–3 1:0.7:0.3; flagellum broken at 11th article; accessory flagellum 1-articulate, minute, slender, one fourth of the length of first flagellum article; sparse setae placed both on peduncle and flagellar articles. *Antenna 2* (Fig. 3; broken in holotype at first peduncular article, description based on paratype): peduncle moderately setose; length of article 4 1.4 × article 5; peduncular article 5 with short setae along dorsal margin; flagellum shorter than peduncle article 5, 7-articulate (but last flagellar articles broken off), sparse setae placed distally on flagellar articles. *Upper lip* (labrum) (Fig. 3): wider than long, rounded apically, with fine setules laterally. *Mandible* (Fig. 3): incisor margins with five teeth; left lacinia mobilis five-cusped; right lacinia mobilis narrower with five cusps; accessory spine rows with five-six serrate setae; molar columnar, strongly triturative, denticulate, with one associated seta; palp 3-articulate, article 1 short, article 2 equal in length to article 3, with 9–10 posterodistal setae, article 3 slightly tapering distally, anterior margin with three to four setae, posterior margin with a row of 30 setae of different length. *Lower lip* (Fig. 3): outer lobes broadly rounded, mandibular lobes narrow; inner lobes large, separate. *Maxilla 1* (Fig. 3): inner plate oval, with two distal setae; outer plate with nine acute setal-teeth (three with bifurcate tips); palp 2-articulate, longer than outer plate, slender, rounded apically, article 1 short, length 0.3 × article 2, article 2 with 10–11 apical/subapical setae and two lateral setae. *Maxilla 2* (Fig. 3): left—inner plate shorter than outer, right—plates subequal in length, inner plate slightly tapering distally, width about 1.1 × outer, with setae and spines apically and subapically, fine setules along inner margin; outer plate rounded with apical spines and setae, with four apicolateral setae. *Maxilliped* (Fig. 4) (due to very strong staining of the holotype during preparation for CLSM some setae, especially placed on the surface of maxilliped not visible): inner plate subrectangular, reaching about 0.3 × basal article of palp, apical margin with eight slender spines; outer plate slender and slightly curved, long, reaching almost 0.5 × length of palp article 2, apical and medial margins with setae and small spines; palp 4-articulate, strong; surface

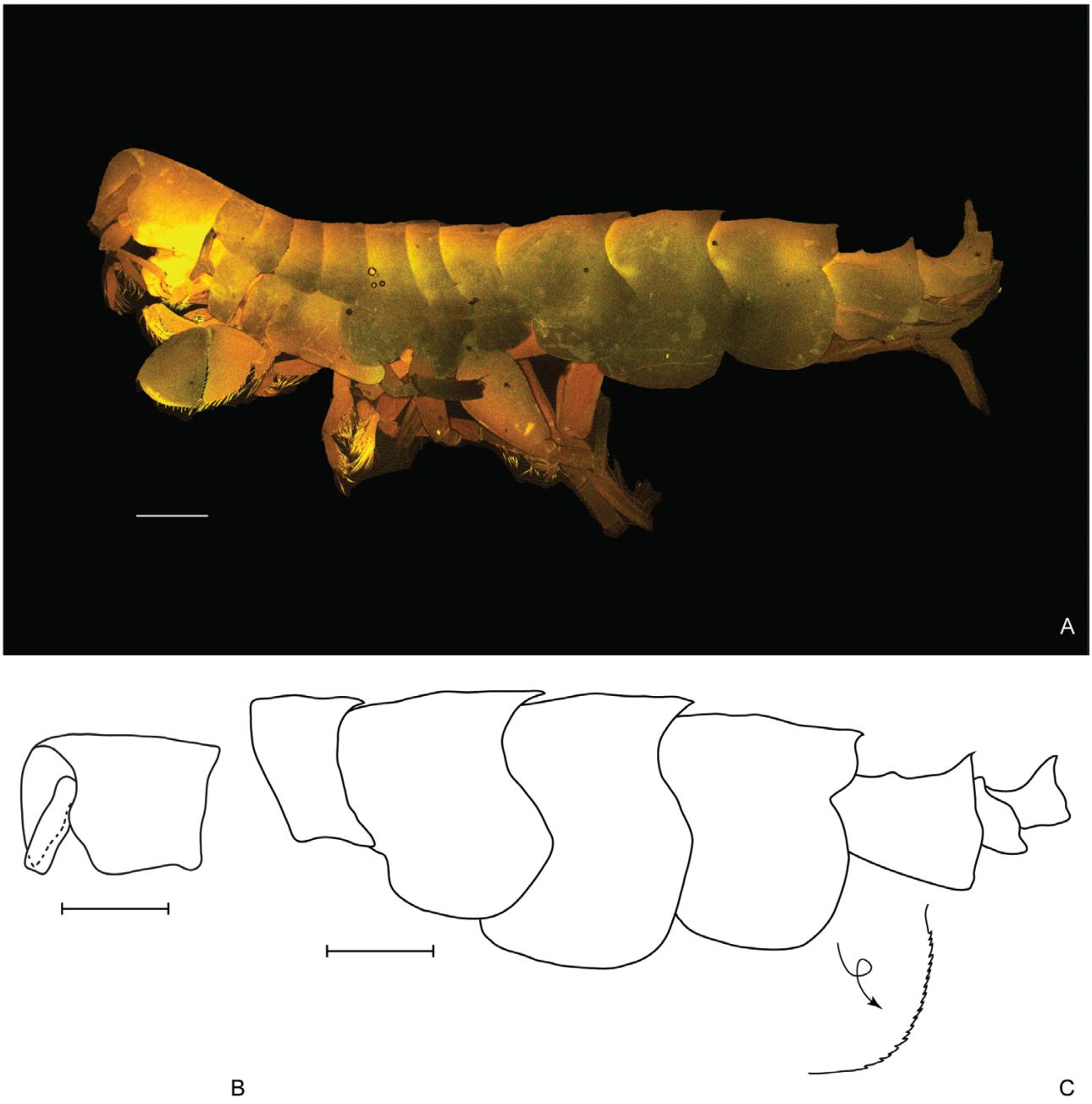

Figure 2. ***Oedicerina henrici*** **sp. nov.** Holotype male (ZMH K-60658, DSB_3762). A, habitus. B, head. C, pereonite 7, pleonites and urosomites, the arrow indicates close up of the epimeral plate 3 margin. Scale bar = 0.5 mm.

of article 2 with minute, triangular scales; article 1 slightly tapering distally; article 2 triangular, widest at the midpoint, with strong medial setae; article 3 expanded mediodistally, but not produced along article 4; article 4 strong, slightly curved; length ratios of articles 1–4 1:1.7:0.7:1.

Pereon. *Pereonite* 1 (Fig. 2) longer than 2, pereonite 3 same length as 2; pereonites 4–5 successively longer; pereonite 6 shorter than pereonite 5, pereonite 7 the longest, extending dorsally into sharp posteriorly directed tooth. *Gnathopod 1* (Fig. 4): coxa subtriangular, distinctly produced anteriorly, anterodistal corner narrowly rounded, posterodistal corner rectangular, ventral margin naked, width to depth ratio 1:0.7; basis straight, weakly expanded, distal half of anterior margin with four long setae and *c.* 10 moderately long setae, posterior margin

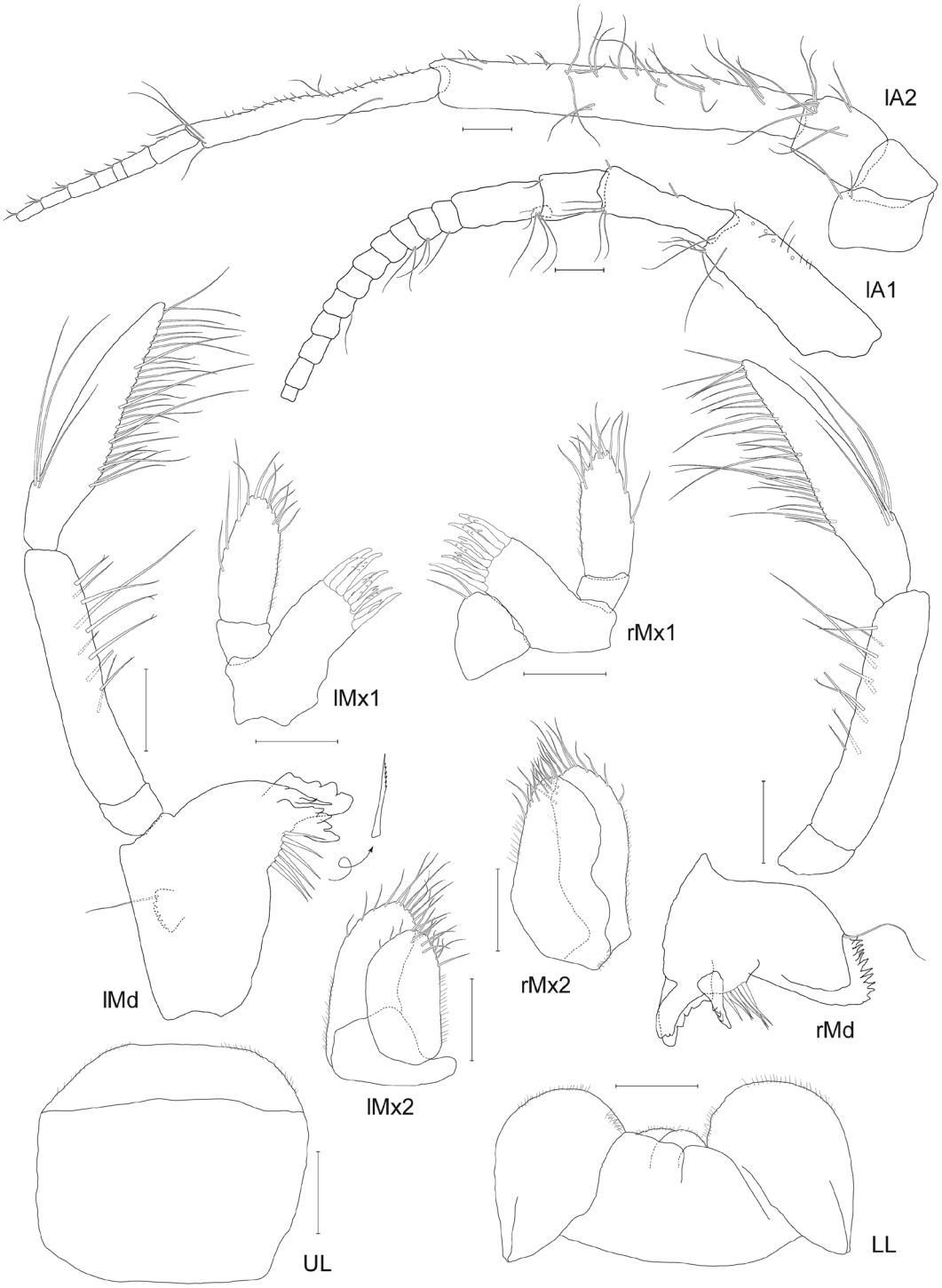

Figure 3. ***Oedicerina henrici*** **sp. nov.** Holotype male (ZMH K-60658, DSB_3762): lMx1, left maxilla 1; rMx1, right maxilla 1; lMd, left mandible; rMd, right mandible; UL, upper lip; lMx2, left maxilla 2; rMx2, right maxilla 2; LL, lower lip. Paratype immature male (ZMH K-60659, DSB_3682): lA1, right antenna 1; lA2, right antenna 2. Scale bar = 0.1 mm, not all setae and spines shown for clarity.

Figure 4. ***Oedicerina henrici*** **sp. nov.** Holotype male (ZMH K-60658, DSB_3762): Mxp, maxilliped; rG1, right gnathopod 1; rc2, right coxa 2. Scale bar = 0.1 mm, not all setae shown for clarity.

without setae, single spine at posterodistal corner; merus, posterodistal lobe rounded, moderately setose; carpus strongly expanded, anterior margin naked, posterior lobe subacute with setae along posterior margin and a few setae placed at distal margin; propodus subchelate, triangular, strongly widening distally, anterior margin with four setae in two groups, palm slightly shorter than hind margin,

transverse, convex, margin crenate, with fine denticulations, with medial spines and lateral row of submarginal setules, palmar corner subrectangular with single spine; dactylus curved, longer than palm. *Gnathopod 2* (Figs 4, 5) (broken in holotype at basis; described based on paratype): coxa narrow, slightly tapering distally, width 0.7 × depth, apex rounded, ventral margin naked; basis straight, six thin setae at inner surface of anterior margin, 20 long setae forming circular patch anterodistally, posterior margin with two moderately long setae, single spine at posterodistal corner; merus, posterodistal lobe narrow, moderately setose; carpus strongly expanded, wider than propodus, anterior margin with a few sparsely placed setae, posterodistal lobe subacute, exceeding palm of propodus, distal margin oblique armed with a row of spines, posterior margin with moderately long setae; propodus shorter than carpus, subchelate, triangular, strongly widening distally, anterior margin with six long setae regularly placed, palm shorter than hind margin, transverse, convex, margin crenate, with fine denticulations, with medial spines and lateral row of submarginal setules, palmar corner subrectangular with single spine; dactylus curved, longer than palm. *Pereopod 3* (Fig. 5): coxa subrectangular, slightly larger than coxa 2, ventral margin naked; basis long and narrow, length 4.5 × width, posterior margin with traces of three short setae, single short spine at posterodistal corner; merus expanded distally, almost naked; carpus length 1.2 × merus, posteriorly armed with long setae organized in eight groups; propodus length 0.6 × carpus, with three groups of long setae anterodistally and *c.* 15 moderately long setae along posterior margin; dactylus thin, shorter than propodus (0.7 × propodus). *Pereopod 4* (Fig. 6): right—coxa wider than deep, anterior margin slightly convex, posteroventral lobe huge, blunt, slightly narrowing distally (width to depth ratio of the lobe 1:0.5), posterior margin deeply excavated; basis long and narrow, length 5.8 × width, single short spine at posterodistal corner; merus weakly expanded; carpus-dactylus broken off; left—coxa partially damaged, not dissected; basis long and narrow, length 6 × width, two short setae along posterior margin, single short spine at posterodistal corner; merus weakly expanded; carpus subequal in length to merus, posteriorly armed with long setae organized in eight groups; propodus length 0.6 × carpus, with three groups of long setae anterodistally and long setae along posterior margin; dactylus slender, shorter than propodus (0.8 × propodus). *Pereopod 5* (Fig. 6): coxa bilobed (partly broken); basis narrow, length 3.4 × width, traces of nine setae along distal half of anterior margin, two short setae at anterodistal corner; merus length 0.9 × basis, with traces of four setae along anterior margin; carpus 0.5 × length of merus armed with 13 setae organized in four groups along posterior margin; propodus slender, 1.1 × length of merus, with groups of setae at posterior margin and at lateral surface; dactylus slender, length 0.7 × propodus. *Pereopod 6* (Fig. 6): coxa bilobed but anterior lobe very small, posterior lobe long, distal margin slightly convex; basis narrow, length 3.1 × width, traces of nine setae along distal half of anterior margin, one short seta at anterodistal corner; merus length 0.7 × basis; carpus-dactylus broken off. *Pereopod 7* (Fig. 6): coxa wider than deep, rounded posteriorly; basis ovate, length 1.7 × width, tapering distally, anterior margin strongly convex with a few sparse short setae, posterior margin rather straight, crenate, posterodistal lobe absent; merus as long as basis with a few setae along anterior and posterior margins; carpus-dactylus broken off.

Pleon. Pleonites 1–2 (Fig. 2) with mid-dorsal, relatively long posteriorly directed teeth; pleonite 3 with short, slender, posteriorly directed tooth. *Epimera*: 1–3 evenly rounded, epimeron 3 crenulated. *Pleopods* [pleopod 2 (Fig. 6)]: powerful, peduncles and rami long.

Urosome. Urosomite 1 (Fig. 2) longest, with a small hump on dorsal surface in the mid length of the urosomite and a distinct, sharp upright tooth at the posterior margin; urosomite 3 longer than 2, depressed anteriorly, with acute mid-dorsal projection over telson. *Uropods*: damaged. *Telson* (Fig. 6): short, length 1.4 × width, cleft 45%, lobes apically damaged, widely diverging, with one seta on dorsal surface.

Intraspecific variation: Due to the bad condition of the individuals not much can be said about sexual or size-dependent dimorphism within the studied species. The only observed difference is the smaller size of the posterodorsal tooth on pleonite 3 in the immature male.

Molecular identification: Following the definition given by Pleijel *et al.* (2008), the sequence of the holotype male of *O. henrici* (ZMH K-60658, GenBank accession number MW377935) is designed as a hologenophore of all obtained sequences. The sequences of the paratype and an additional individual of the species are deposited in GenBank with the following accession numbers: MW377932, MW377937. The species has also received a Barcode Index Number from BOLD: AEB1524 (dx.doi.org/10.5883/BOLD:AEB1524).

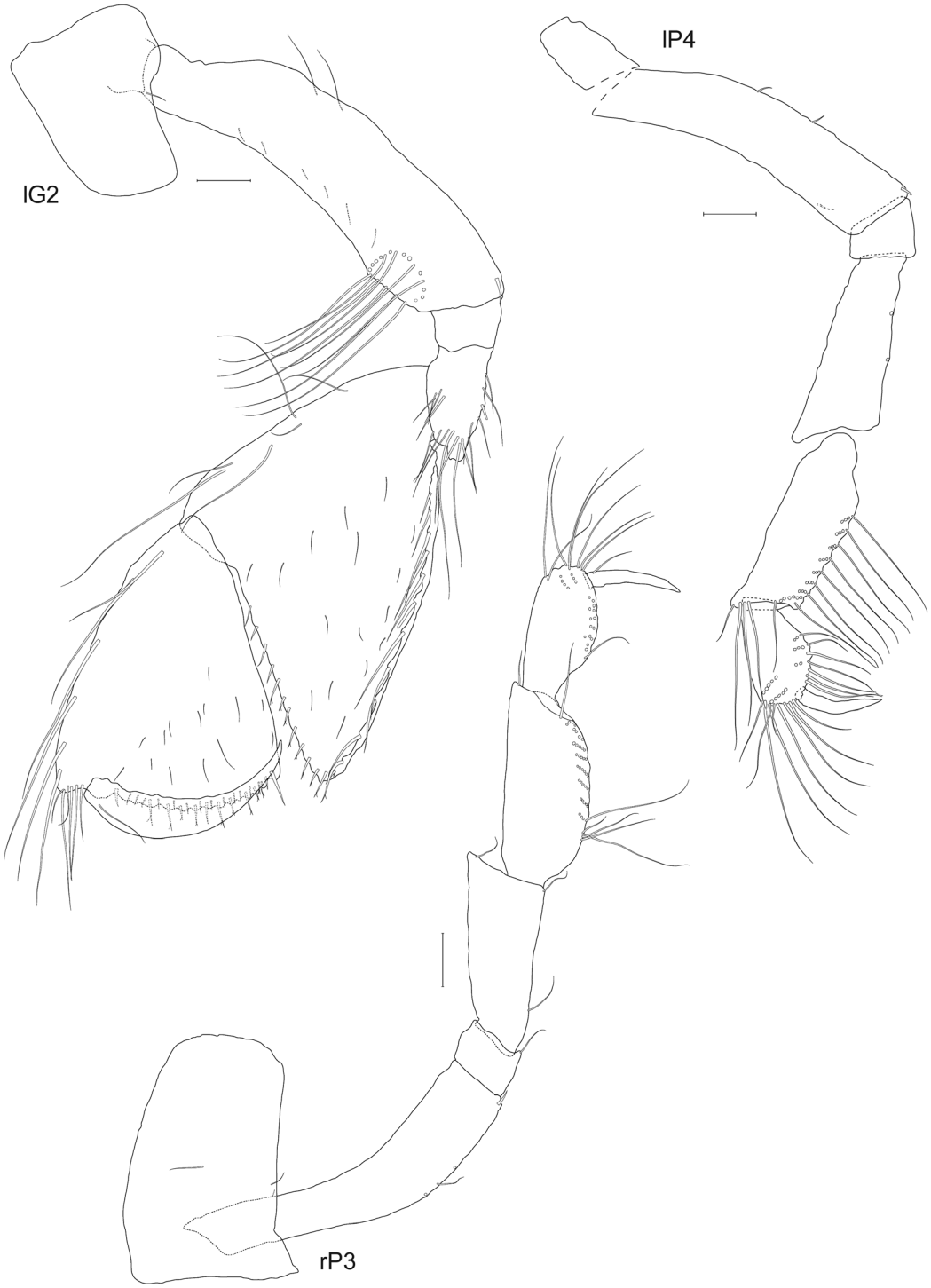

Figure 5. ***Oedicerina henrici*** **sp. nov.** Holotype male (ZMH K-60658, DSB_3762): rP3, right pereopod 3; lP4, left pereopod 4. Paratype immature male (ZMH K-60659, DSB_3682): lG2, left gnathopod 2. Scale bar = 0.1 mm, not all setae shown for clarity. The dashed line (long dashes) indicates the place where the appendage was damaged.

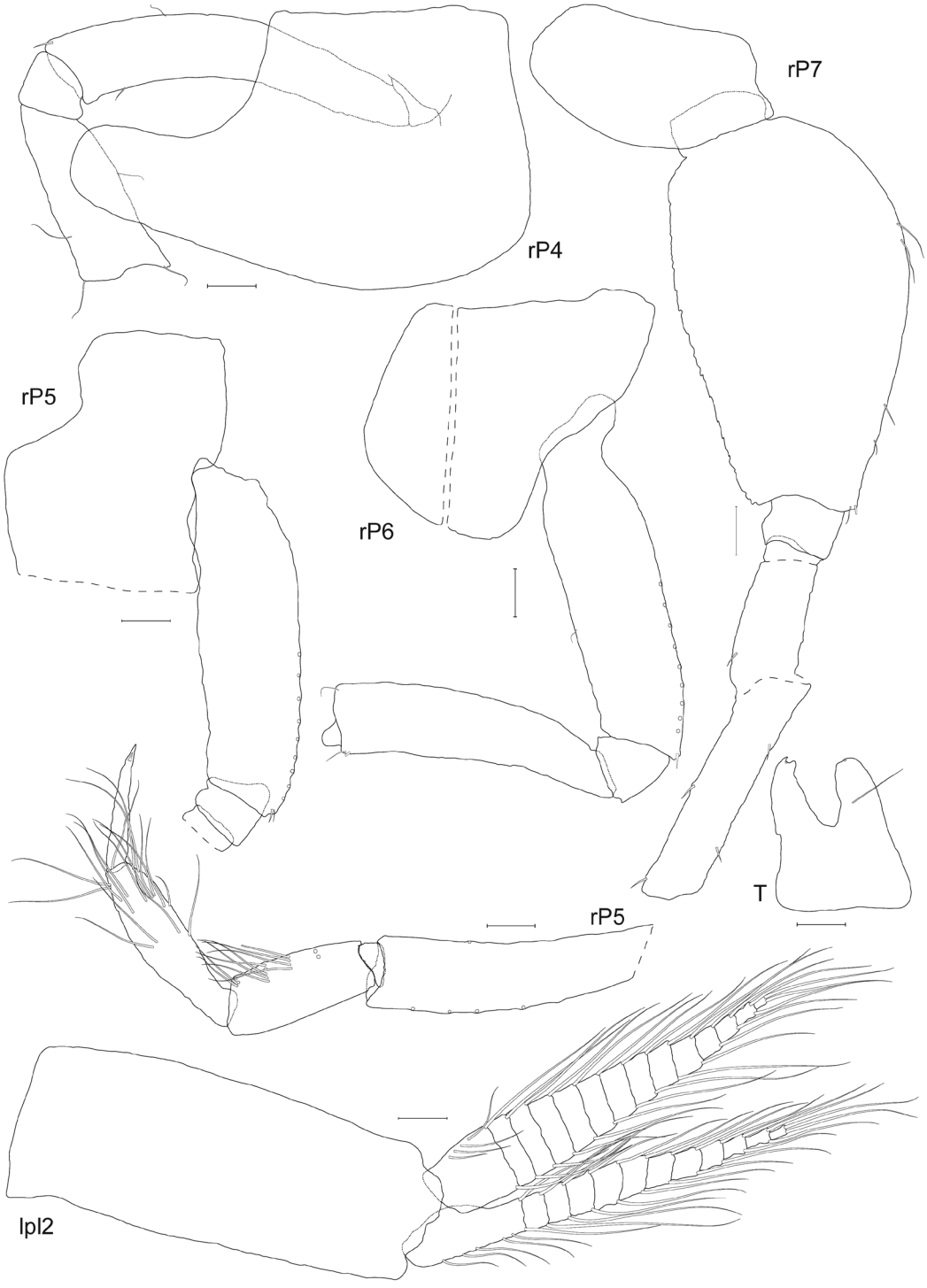

Figure 6. ***Oedicerina henrici*** **sp. nov.** Holotype male (ZMH K-60658, DSB_3762): rP4–rP7, right pereopod 4–7, respectively; lpl2, left pleopod 2; T - telson. Scale bar = 0.1 mm. The dashed line (long dashes) indicates the place where the appendage was damaged.

Distribution: Eastern central Pacific, CCZ (Fig. 25), 4111–4359 m.

OEDICERINA TERESAE JAŻDŻEWSKA, SP. NOV.

(FIGS 7–12)

Zoobank registration: urn:lsid:zoobank.org:act:8B11C501-328E-4F33-AA78-F2229D4847A1.

Type material

Holotype: Immature ♂, 5.5 mm, body remnants and two slides with appendages, ZMH K-60661, DSB_3680, St. Ma 16–25, 11°49.143' N, 116°58.492' W-11°49.975' N, 116°57.797' W; 4107–4101 m, 29 April 2016, leg. Annika Janssen.

Allotype: Mature ♀ (oostegites setose, no egg), 5.8 mm, ZMH K-60662, DSB_3818, St. AB2-EB12, 12°02.72' N, 117°25.43' W-12°03.03' N, 117°24.28' W; 4223–4299 m, 16 March 2015, leg. Inga Mohrbeck.

Paratype: One juvenile, 3.4 mm, ZMH K-60663, DSB_3681, St. Ma 16–28, 11°49.654' N, 117°00.299' W-11°49.902' N, 116°59.174' W; 4143–4133 m, 1 May 2016, leg. Annika Janssen.

Additional material: One individual sex undetermined, broken in two parts, DNA extracted from anterior part, posterior part preserved but not used for taxonomic evaluation, ZMH K-60664, DSB_3683, St. Ma 16–95, 11°47.862' N, 117°30.639' W-11°47.152' N, 117°29.490' W, 4356–4359 m, 9 May 2016, leg. Annika Janssen.

The registered type material is deposited in the Zoological Museum of Hamburg, Germany.

Type locality: Eastern central Pacific, CCZ, St. Ma 16–25, 11°49.143' N, 116°58.492' W-11°49.975' N, 116°57.797' W; 4107–4101 m.

Etymology: The species is named for Dr. Teresa Jażdżewska, the first author's mother and a specialist in ephemeropteran and hirudinean taxonomy, diversity and ecology.

Description: Based on male, 5.5 mm, St. Ma 16–25. *Head* (Fig. 7): longer than deep, longer than pereonites 1–2 combined; no eyes or ocular pigment visible; rostrum curved but not deflexed, the angle between head dorsal margin and rostrum margin more than 90 °, rostrum reaching 2/3 of first article of peduncle of antenna 1; interantennal lobe moderate, subtriangular. *Antenna 1* (Fig. 8): subequal in length to antenna 2; length ratios of peduncle articles 1–3 1:0.7:0.4; flagellum 12-articulate, first article longer than article 3 of peduncle; accessory flagellum 1-articulate, minute, slender, length 0.1 × first flagellum article; peduncle sparsely setose, flagellum naked. *Antenna 2* (Fig. 8): peduncle moderately setose; length of article 4 0.9 × article 5; flagellum broken at sixth article (right antenna 2–7-articulate). *Upper lip* (labrum) (Fig. 8): damaged during preparation. *Mandible* (Fig. 8): incisor margins with five (left) or six (right) teeth; left lacinia mobilis six-cusped; right lacinia mobilis narrower with four cusps; accessory spine rows with four slender, pectinate spines; molar columnar, strongly triturative, denticulate, with one associated seta; palp 3-articulate, article 1 short, article 2 length 0.7 × article 3, with seven posterodistal setae, article 3 slightly tapering distally, anterior margin with three (left) or four (right) setae, posterior margin with 11 setae, apically with two or three setae. *Lower lip* (Fig. 8): outer lobes broadly rounded, mandibular lobes narrow; inner lobes large, separate. *Maxilla 1* (Fig. 8): inner plate oval, with two distal setae; outer plate with eight acute setal-teeth (three/four with bifurcate tips); palp 2-articulate, longer than outer plate, robust, rounded apically, article 1 short, length 0.25 × article 2, article 2 with eight apical/subapical setae and one long, lateral setae. *Maxilla 2* (Fig. 8): inner plate wider than outer, right inner plate also shorter than outer (left subequal in length), inner plate with setae and spines apically and subapically, fine setules along inner and outer margins; outer plate rounded with apical spines and setae, with one moderately long apicolateral setae. *Maxilliped* (Fig. 9): inner plate subrectangular, reaching about 0.3 × basal article of palp, apical margin with seven slender spines; outer plate slender and slightly curved, long, reaching 0.5 × length of palp article 2, apical and medial margins with setae and small spines; palp 4-articulate, strong; article 1 tapering distally; article 2 triangular, widest at the midpoint, with strong medial setae; article 3 expanded mediodistally, not produced along article 4; article 4 strong, slightly curved; length ratios of articles 1–4 1:1.8:0.7:1.

Pereon. Pereonite 1 (Fig. 7) longer than pereonite 2, pereonites 3–6 of similar length, longer than 2, pereonite 7 the longest, extending dorsally into a sharp posteriorly directed tooth. *Gnathopod 1* (Fig. 9): coxa subtriangular, anterodistal corner subacute, posterodistal corner rectangular, ventral margin with single short seta anteriorly placed, width to depth ratio 1:1; basis straight, slightly expanded distally, distal half of anterior margin with row of long setae, posterior margin with long setae (some delicately plumose), posterodistal corner with single spine, some short setae on the inner surface; merus, posterodistal lobe rounded, moderately setose; carpus strongly expanded, anterior margin with six setae along distal half (some delicately plumose), posterior lobe rounded with setae along posterior and distal margins; propodus subchelate,

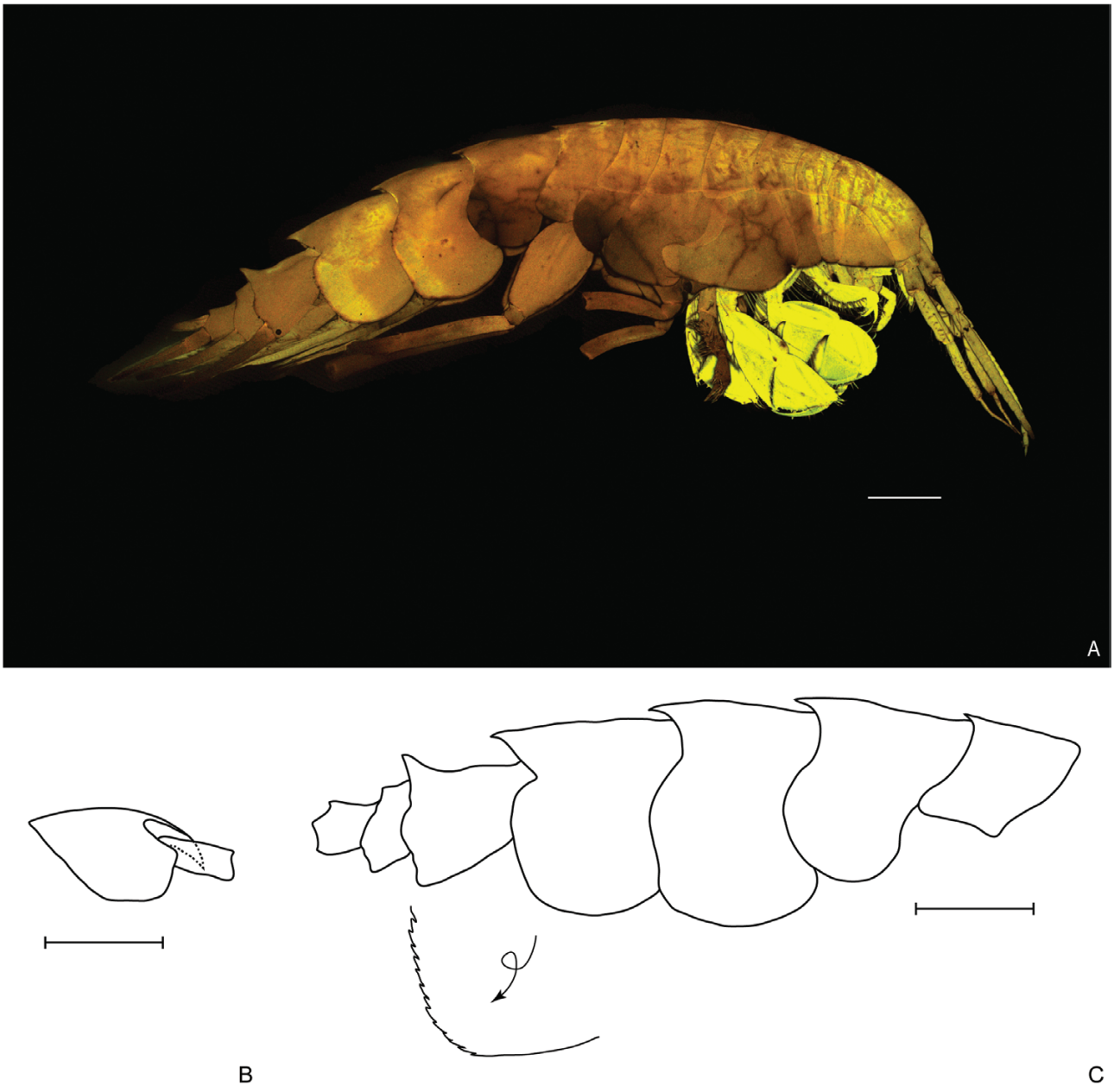

Figure 7. ***Oedicerina teresae*** **sp. nov.** Holotype male (ZMH K-60661, DSB_3680). A, habitus. B, head. C, pereonite 7, pleonites and urosomites, the arrow indicates close up of the epimeral plate 3 margin. Scale bar = 0.5 mm.

triangular, strongly widening distally, anterior margin moderately setose, palm almost as long as hind margin, transverse, convex, margin crenate, with fine denticulations, with medial spines and lateral row of submarginal setules, palmar corner subrectangular with one spine; dactylus curved, distinctly longer than palm. *Gnathopod 2* (Fig. 10): coxa narrow, slightly tapering distally, width 0.5 × depth, apex rounded, ventral margin naked; basis straight, *c.* 15 long setae forming circular patch anterodistally, four long setae at posterior margin, three setae at posterodistal corner, some setae at the surface; merus, posterodistal lobe narrow, subacute, moderately setose; carpus strongly expanded, wider than propodus, anterior margin with two setae, posterodistal lobe subacute, extending palmar corner of propodus, distal margin oblique armed with a row of spines, posterior margin with moderately long setae; propodus longer than carpus, subchelate, triangular, strongly widening distally, anterior margin with four long setae regularly placed,

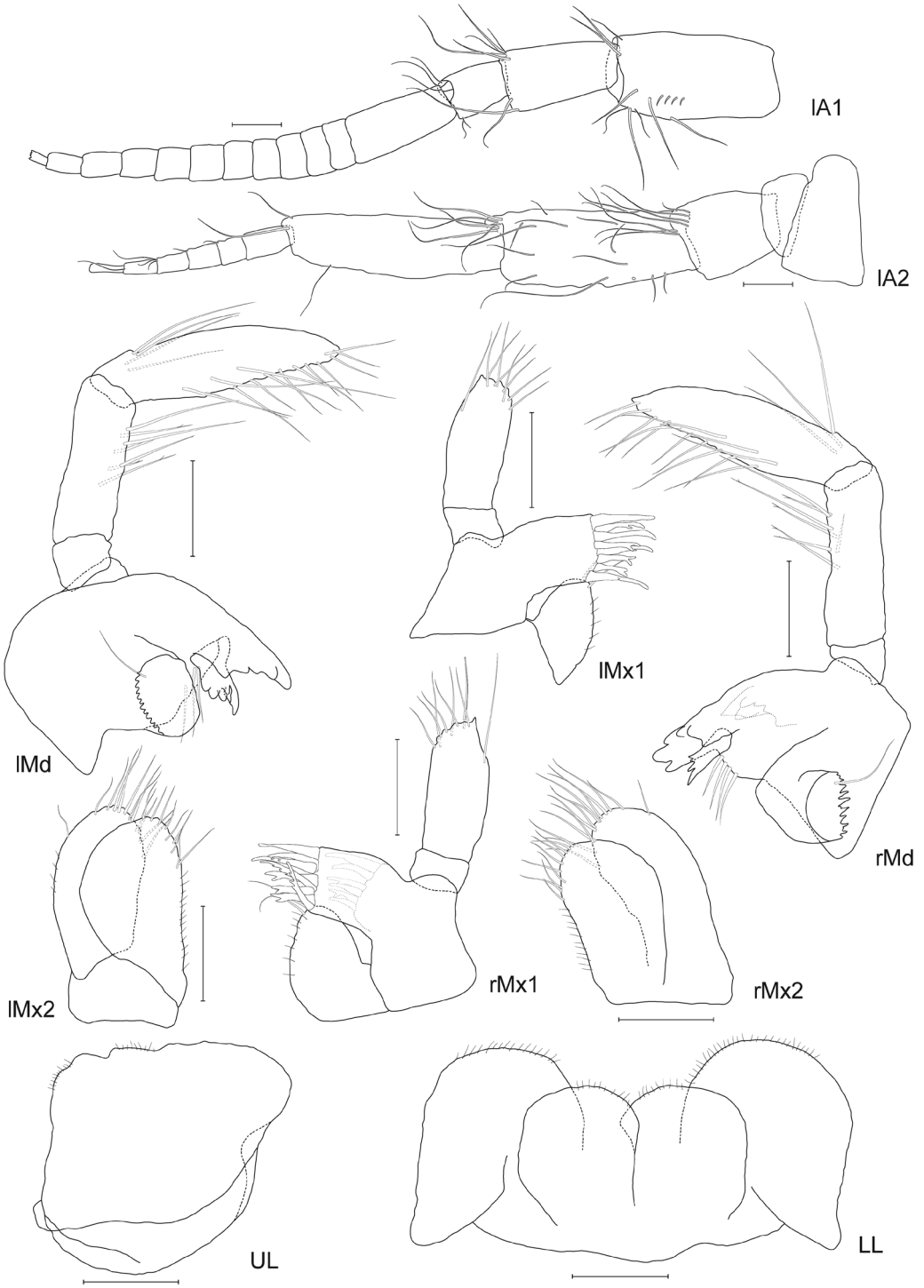

Figure 8. ***Oedicerina teresae*** **sp. nov.** Holotype male (ZMH K-60661, DSB_3680): lA1, left antenna 1; lA2, left antenna 2; lMx1, left maxilla 1; rMx1, right maxilla 1; lMd, left mandible; rMd, right mandible; UL, upper lip; lMx2, left maxilla 2; rMx2, right maxilla 2; LL, lower lip. Scale bar = 0.1 mm, not all setae and spines shown for clarity.

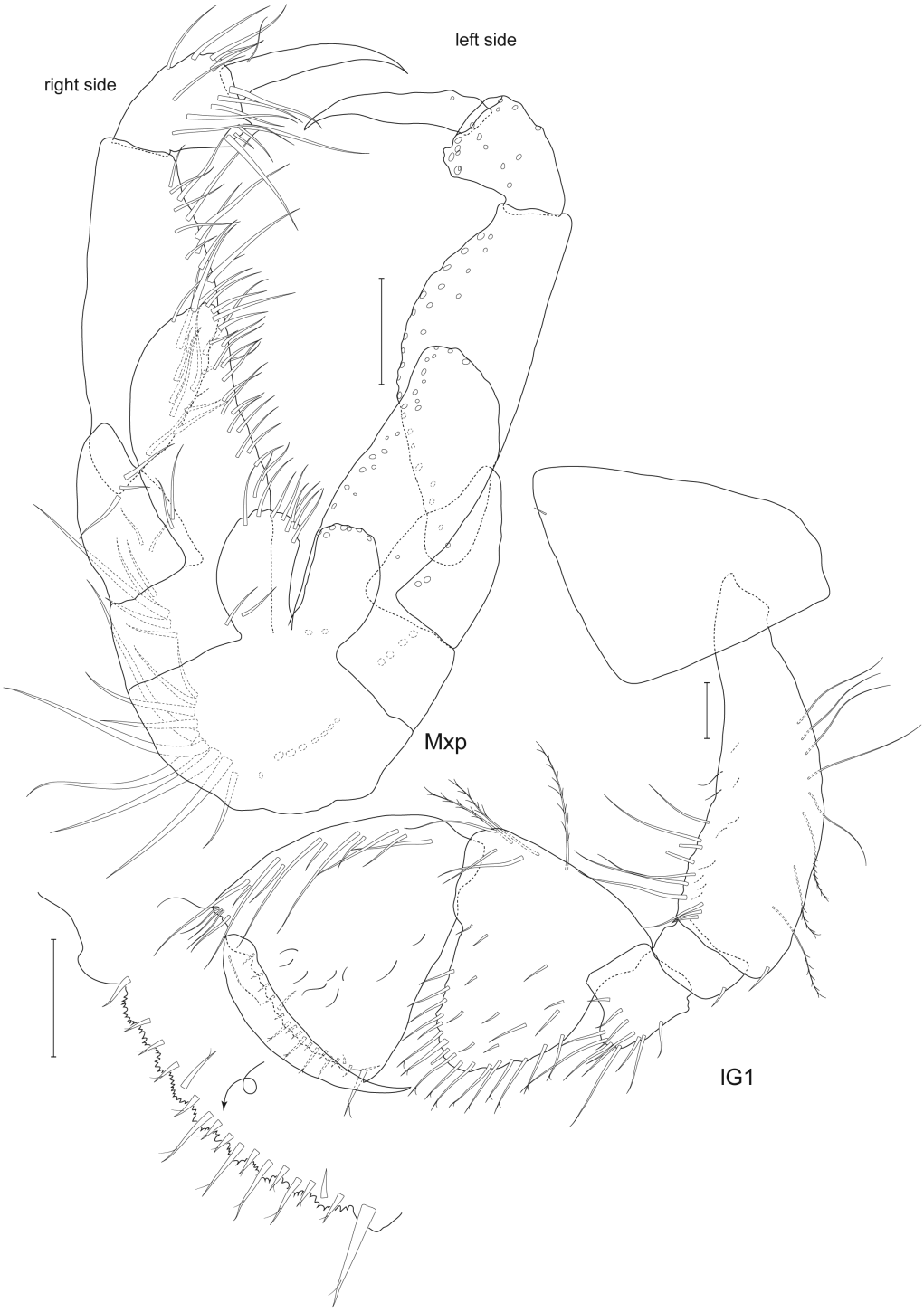

Figure 9. ***Oedicerina teresae*** **sp. nov.** Holotype male (ZMH K-60661, DSB_3680): Mxp, maxilliped; lG1, left gnathopod 1. Scale bar = 0.1 mm, not all setae shown for clarity.

group of setae at anterodistal corner, palm shorter than hind margin, transverse, convex, margin crenate, with fine denticulations, with medial spines and lateral row of submarginal setules, palmar corner subrectangular with one spine; dactylus curved, just longer than palm. *Pereopod 3* (Fig. 10): coxa subrectangular, wider and deeper than coxa 2, ventral margin naked; basis longer than coxa, narrow, length 5.4 × width, some long

Figure 10. ***Oedicerina teresae*** **sp. nov.** Holotype male (ZMH K-60661, DSB_3680): lG2, right gnathopod 2; lP3, left pereopod 3; lP4, left pereopod 4. Scale bar = 0.1 mm, not all setae shown for clarity.

setae anteriorly; merus slightly expanded distally, two groups of setae anterodistally and three groups of setae posteriorly; carpus narrow, length 1.1 × merus, one group of setae at anterodistal corner, posteriorly armed with long setae organized in eight groups; propodus length 0.6 × carpus, with a group of setae anterodistally and five groups of moderately long setae along posterior margin; dactylus thin, as long as propodus.

Pereopod 4 (Fig. 10): coxa wider than deep, anterior margin strongly convex, extending distally, coxa the widest almost at 2/3 of its depth, ventral margin naked, posteroventral lobe huge, blunt (width to depth ratio of the lobe 1:0.7), posterior margin deeply excavated; basis long and narrow, length 5.4 × width, sparse long setae at anterior and posterior margin as well as on the surface; merus slightly expanded, sparsely setose; carpus-dactylus broken off. *Pereopod 5* (Fig. 11): coxa about as deep as coxa 4, bilobed, posterior lobe expanded ventrally, ventral margin straight, with one seta anteriorly placed, anterior lobe 0.5 × depth of posterior lobe; basis narrow, length 2.8 × width, five long, delicately plumose setae at anterior margin, three long setae along posterior margin; merus as long as basis, sparsely setose; carpus-dactylus broken off. *Pereopod 6* (Fig. 11): coxa partly damaged; basis narrow, length 3.3 × width, sparsely setose; merus as long as basis, sparsely setose; carpus-dactylus broken off. *Pereopod 7* (Fig. 11): coxa wider than deep, rounded posteriorly; basis ovate, length 1.6 × width, widest in the mid length, tapering distally, anterior margin strongly convex, one short spine at anterodistal corner, posterior margin slightly oblique in distal half, denticulate,

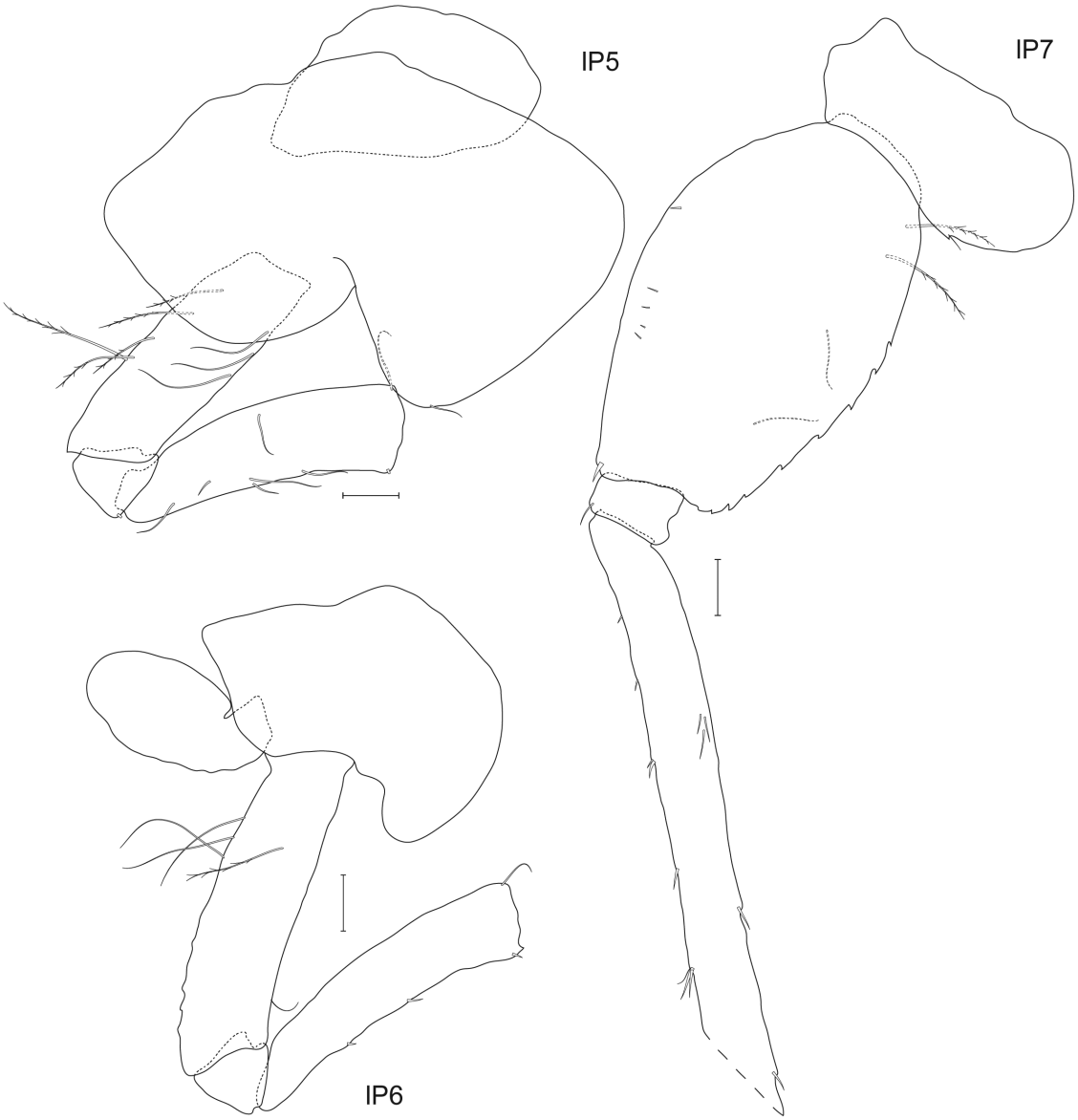

Figure 11. ***Oedicerina teresae*** **sp. nov.** Holotype male (ZMH K-60661, DSB_3680): lP5–7, left pereopod 5–7, respectively. Scale bar = 0.1 mm, not all setae shown for clarity. The dashed line (long dashes) indicates the place where the appendage was damaged.

posterodistal lobe absent; merus distally damaged, with groups of setae both anteriorly and posteriorly (some setae broken); carpus-dactylus broken off.

Pleon. *Pleonites* 1–3 (Fig. 7) with distinct mid-dorsal, posteriorly directed teeth. *Epimera*: 1 and 3 evenly rounded, epimeron 2 posterodistal corner subquadrate, epimeron 3 delicately serrate. *Pleopods* [pleopod 1 (Fig. 12)]: powerful, peduncles and rami long.

Urosome. *Urosomite* 1 (Fig. 7) longest, produced distally into a sharp, large, upright tooth; urosomite 3 longer than 2. *Uropods* (Fig. 12): *Uropod 1* (damaged): peduncle margins with some moderately long setae; rami broken off. *Uropod 2* (rami damaged): peduncle with some moderately long setae; inner ramus with sparse setae. *Uropod 3:* peduncle short, peduncle length 0.3 × inner ramus; inner and outer ramus with short spines along lateral margins. *Telson*: (Fig. 12) short, length 1.5 × width, cleft 35%, lobes subacute, widely diverging, notched subapically, tips unequal in size (inner slightly shorter than outer; on one side outer tip broken), single seta placed in the notch.

Intraspecific variation: No distinct differences were observed between the holotype and the mature female collected. The difference between adult individuals and the juveniles is expressed by the number of articles of flagella of antenna 1 and antenna 2 which is smaller in the latter.

Molecular identification: Following the definition given by Pleijel *et al.* (2008), the sequence of the holotype male of *O. teresae* (ZMH K-60661, GenBank accession number MW377944) is designed as a hologenophore of all obtained sequences. The sequences of the paratype and additional individuals of the species are deposited in GenBank with the following accession numbers: MW377925, MW377934, MW377942. The species has received also a Barcode Index Number from BOLD: AEB1523 (dx.doi.org/10.5883/BOLD:AEB1523).

Distribution: Eastern central Pacific, CCZ (Fig. 25), 4101–4359 m.

OEDICERINA LESCI JAŻDŻEWSKA, SP. NOV.

(FIGS 13–18)

Zoobank registration: urn:lsid:zoobank.org:act:8242F310-A152-4CB7-8BE3-EAAF8A848D9A.

Oedicerotidae sp. 10 Jażdżewska, 2015

Oedicerina sp. Golovan *et al.*, 2019 (excluding one individual from station 2–9 and one in dividual from station 5–10).

Oedicerina sp. 1 Jażdżewska & Mamos, 2019

Type material

Holotype: ♀, 13.6 mm, body remnants and two slides with appendages, SMF-56780, SB_10-7E_Oedi10_2015_1, St. AKL-71-10-7, 46°06.027’ N, 152°14.439’ E-46°05.827’ N, 152°14.576’ E; 4769–4798 m, 29 July 2015, leg. Marina V. Malyutina.

Allotype: ♂, 10.0 mm, one slide with appendages, SMF-56779, 3-9S_Oedi10_2012_1, St. SO-223-3-9, 47°14.66’ N, 154°42.88’ E-47°14.76’ N, 154°43.03’ E; 4987–4991 m, 5 August 2012, leg. Angelika Brandt.

Paratypes: ♀, 9.0 mm, MIMB 40714, 3-9S_Oedi10_2012_2, St. SO-223-3-9, 47°14.66’ N, 154°42.88’ E-47°14.76’ N, 154°43.03’ E; 4987–4991 m, 5 August 2012, leg. Angelika Brandt.

♂, 9.2 mm, MIMB 40715, SB_10-7S_Oedi10_2015_2, St. AKL-71-10-7, 46°06.027’ N, 152°14.439’ E-46°05.827’ N, 152°14.576’ E; 4769–4798 m, 29 July 2015, leg. Marina V. Malyutina.

Additional material: One ♀, 8.0 mm, 1-11S_Oedi_2012_1, St. SO-223-1-11, 43°58.44’ N, 157°18.29’ E-43°58.61’ N, 157°18.13’ E; 5418–5419 m, 30 July 2012, leg. Angelika Brandt.

One juvenile, 3.5 mm, 2-9S_Oedi10_2012_1, St. SO-223-2-9, 46°14.78’ N, 155°32.63’ E-46°14.92’ N, 155°32.57’ E; 4830–4863 m, 3 August 2012, leg. Angelika Brandt.

Two ♀, 8.6–12.0 mm, 15 juveniles, 2.8–7.0 mm, St. SO-223-3-9, 47°14.66’ N, 154°42.88’ E-47°14.76’ N, 154°43.03’ E; 4987–4991 m, 5 August 2012, leg. Angelika Brandt.

One juvenile, 5.1 mm, 9-9S_Oedi10_2012_1, St. SO-223-9-9, 40°34.51’ N, 150°59.92’ E-40°34.25’ N, 150°59.91’ E; 5399– 5421 m, 23 August 2012, leg. Angelika Brandt.

One juvenile, 3.6 mm, St. SO-223-10-9, 41°12.80’ N, 150°6.162’ E-41°13.01’ N, 150°05.652’ E; 5245–5262 m, 26 August 2012, leg. Angelika Brandt.

One ♂?, 10.0 mm, SB_10-5E_Oedi10_2015_1, 46°07.410’ N, 152°11.292’ E-46°07.310’ N, 152°11.537’ E; 4681–4702 m, 28 July 2015, leg. Marina V. Malyutina.

Two ♂, 8.5–10.6 mm, St. AKL-71-10-7, 46°06.027’ N, 152°14.439’ E-46°05.827’ N, 152°14.576’ E; 4769–4798 m, 29 July 2015, leg. Marina V. Malyutina.

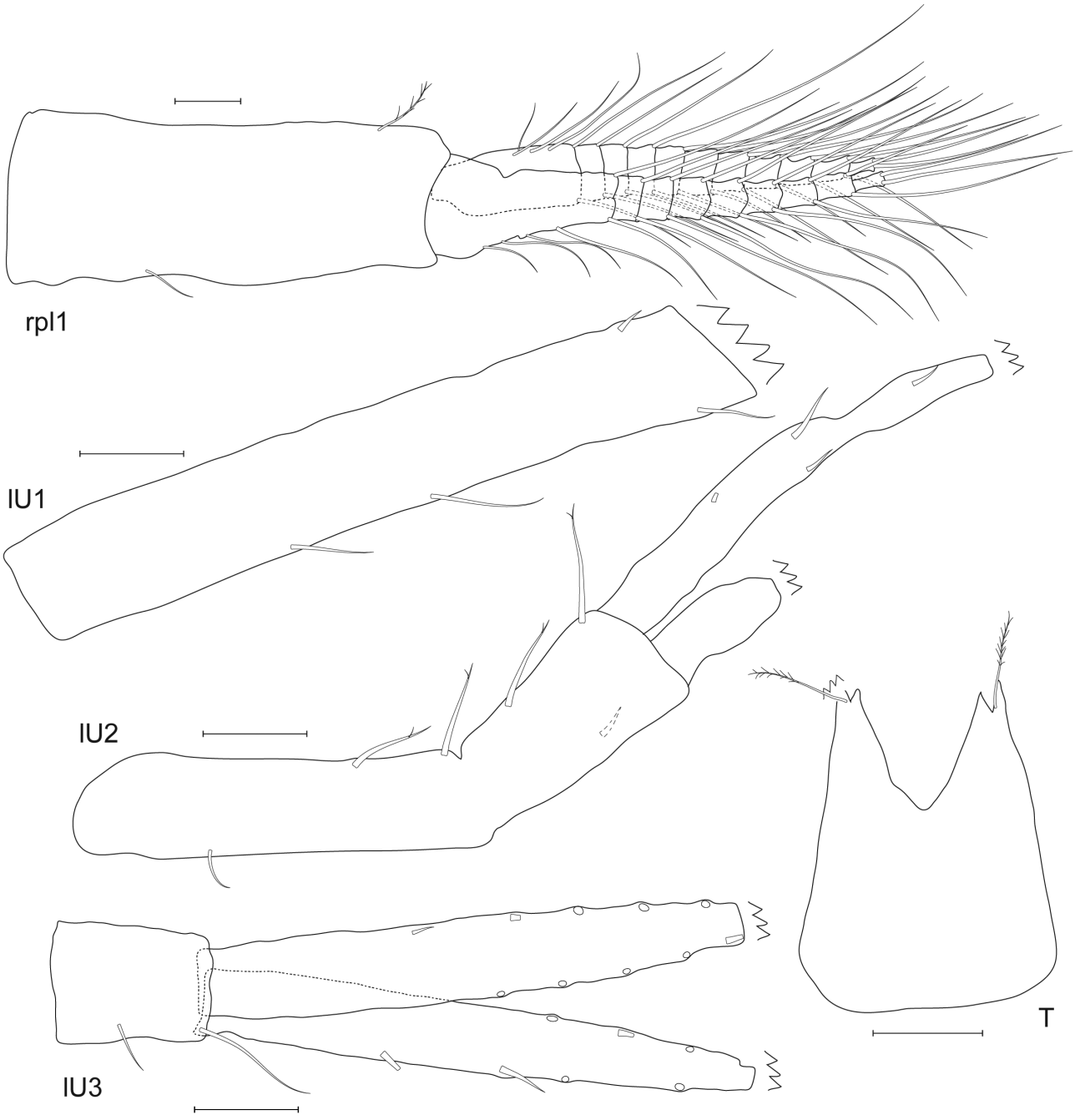

Figure 12. ***Oedicerina teresae*** **sp. nov.** Holotype male (ZMH K-60661, DSB_3680): rpl1, right pleopod 1; lU1–U3, left uropod 1–3, respectively; T, telson. Scale bar = 0.1 mm. The zig-zag line indicates the place where the appendage was damaged.

One immature ♀, 8.5 mm, 85S_Oedi10_2016_1, SO-250–85, 45°02.26' N, 151°02.14' E-45°01.64' N, 151°03.68' E; 4903.4–5265.6 m, 15 September 2016, leg. Angelika Brandt.

The registered type material is deposited in the Senckenberg Museum (SMF; Frankfurt, Germany), and in the National Scientific Center of Marine Biology (MIMB; Vladivostok, Russia). All the remaining material is kept in the scientific collection of the Department of Invertebrate Zoology and Hydrobiology, University of Lodz.

Type locality: Abyssal plain adjacent to the KKT, St. AKL-71-10-7, 46°06.027' N, 152°14.439' E-46°05.827' N, 152°14.576' E; 4769–4798 m.

Etymology: The species is named for Krzysztof Leszek (Latin *Lescus*) Jażdżewski, the first author's brother.

Description: Based on female, 13.6 mm, St. AKL-71-10-7. *Head* (Fig. 13): longer than deep, longer than pereonites 1–3 combined; no eyes or ocular pigment visible; rostrum curved but not deflexed, the angle between head dorsal margin and rostrum margin more than 90 °, rostrum reaching 2/3 of first article of peduncle of antenna 1; interantennal lobe moderate, subtriangular, rounded. *Antenna 1* (Fig. 14): shorter than antenna 2; length ratios of peduncle articles 1–3 1:1:0.6, peduncle article 1 dorsally slightly but acutely produced; flagellum 10-articulate; accessory flagellum 1-articulate, minute, slender, half of the length of first flagellum article; peduncular article 1 moderately setose, peduncular articles 2–3 and flagellar articles with sparse setae. *Antenna 2* (Fig. 14): peduncle setose (especially article 4); length of article 4 1.5 × article 5; flagellum broken at fourth article. *Upper lip* (labrum) (Fig. 14): wider than long, rounded apically, with fine setules laterally. *Mandible* (Fig. 14): incisor margins with five teeth; left lacinia mobilis five-cusped; right lacinia mobilis narrower slightly cuspidate; accessory spine rows with seven serrate setae; molar columnar, strongly triturative, denticulate, with one associated seta; palp 3-articulate, article 1 short, article 2 equal in length to article 3, swollen proximally, with 17–18 posterodistal setae, article 3 slightly tapering distally, anterior margin with two setae, posterior margin with eight to nine setae, apically with two or three setae. *Lower lip* (Fig. 14): outer lobes broadly rounded, mandibular lobes narrow; inner lobes large, separate. *Maxilla 1* (Fig. 14): inner plate oval, with two distal setae; outer plate with nine acute setal-teeth (three with bifurcate tips); palp 2-articulate, longer than outer plate, robust, rounded apically, article 1 short, length 0.3 × article 2, article 2 with 13 apical/subapical setae and two long, lateral setae, lateral margin with row of small spines. *Maxilla 2*

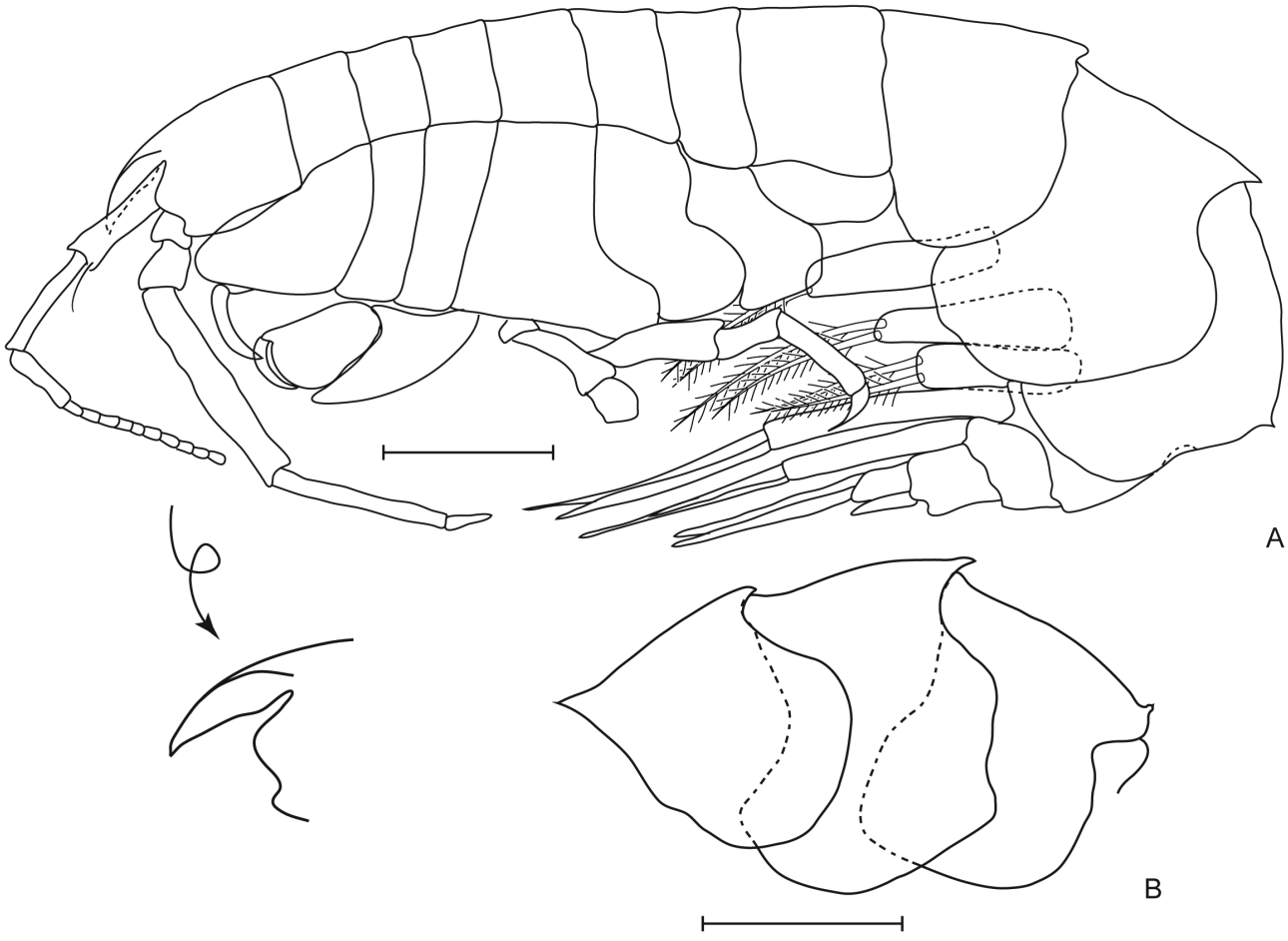

Figure 13. ***Oedicerina lesci* sp. nov.** Holotype female (SMF-56780, 10-7S_Oedi_2015_1). A, habitus. B, pleonites 1–3. Scale bar = 1 mm.

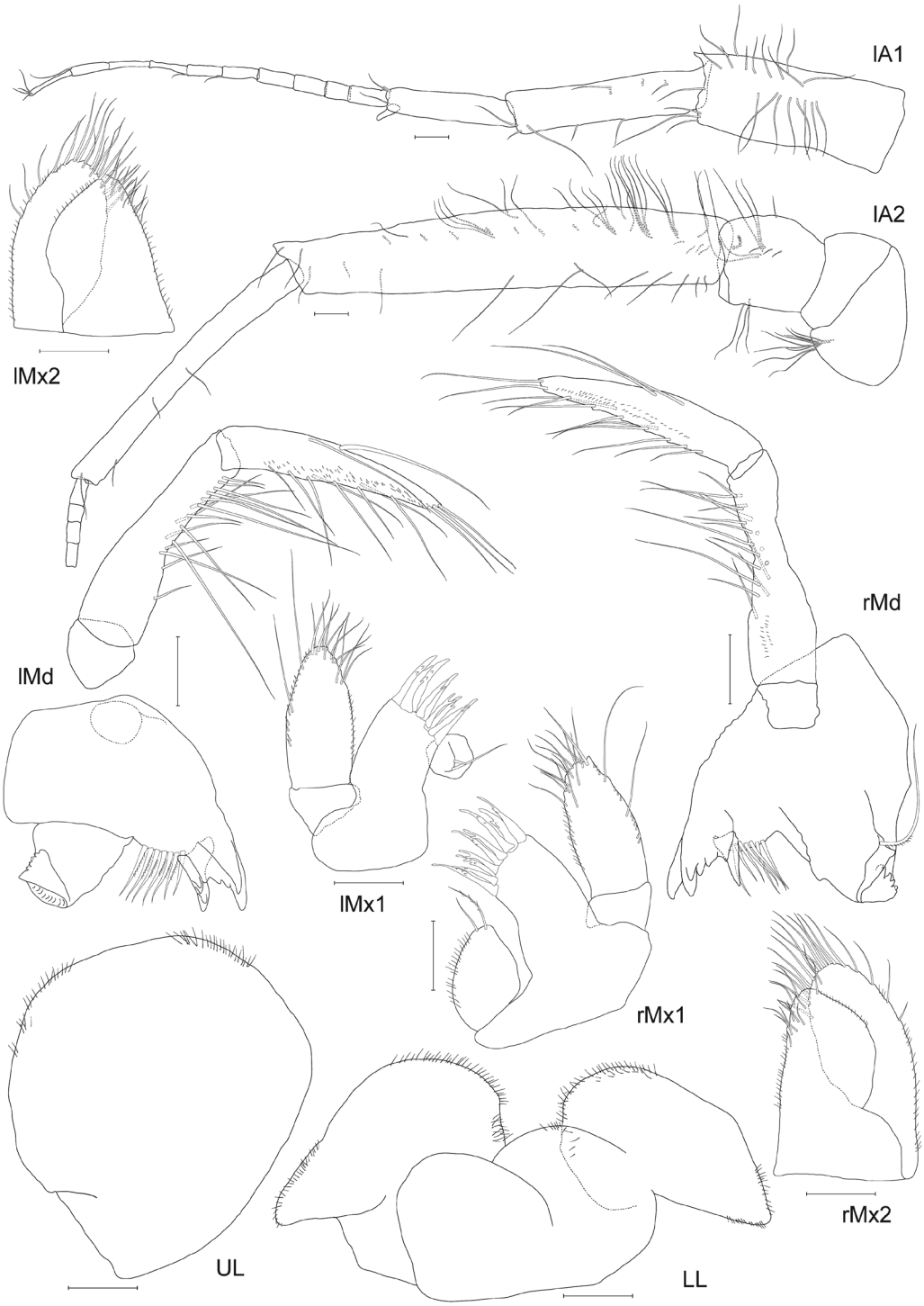

Figure 14. ***Oedicerina lesci*** **sp. nov.** Holotype female (SMF-56780, 10-7S_Oedi_2015_1): lA1, left antenna 1; lA2, left antenna 2; lMx1, left maxilla 1; rMx1, right maxilla 1; lMd, left mandible; rMd, right mandible; UL, upper lip; lMx2, left maxilla 2; rMx2, right maxilla 2; LL, lower lip. Scale bar = 0.1 mm, not all setae and spines shown for clarity.

(Fig. 14): plates same width, but inner shorter than outer, inner plate slightly tapering distally, with setae and spines apically and subapically, fine setules along inner and outer margins; outer plate rounded with apical spines and setae, with three moderately long apicolateral setae. *Maxilliped* (Fig. 15) (outer plate on the left side damaged): inner plate subrectangular, reaching about 0.3 × basal article of palp, apical

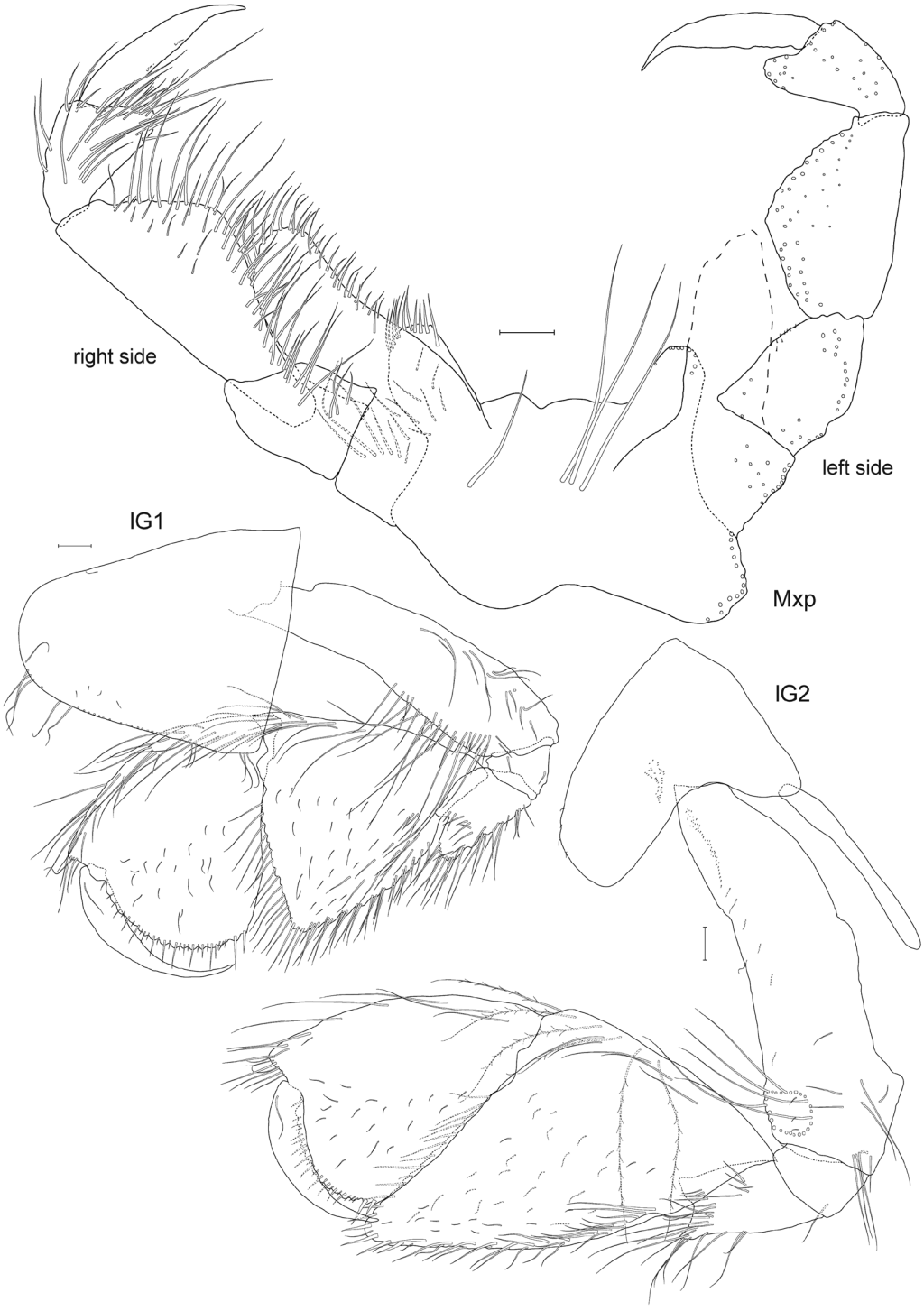

Figure 15. ***Oedicerina lesci*** **sp. nov.** Holotype female (SMF-56780, 10-7S_Oedi_2015_1): Mxp, maxilliped; lG1, left gnathopod 1; lG2, left gnathopod 2. Scale bar = 0.1 mm, not all setae shown for clarity.

margin with ten slender spines; outer plate slender and slightly curved, long, reaching 0.4 × length of palp article 2, apical and medial margins with setae and small spines; palp 4-articulate, strong; article 1 slightly tapering distally; article 2 triangular, widest at the midpoint, with strong medial setae; article 3 expanded mediodistally, produced along article 4; article 4 strong, slightly curved; length ratios of articles 1–4 1:1.8:0.8:1.3.

Pereon. *Pereonites* 1–6 (Fig. 13) of similar length, pereonite 7 distinctly longer. *Gnathopod 1* (Fig. 15): coxa subtriangular, anterodistal corner bluntly rounded, posterodistal corner rectangular, ventral margin setose (some moderately long setae preserved and traces of several broken setae), width to depth ratio 1:0.9; basis straight, weakly expanded, distal half of anterior margin with row of long setae, posterior surface setose; merus, posterodistal lobe rounded, strongly setose; carpus strongly expanded, anterior margin setose along distal half, posterior lobe subacute with setae along posterior margin and distal margin; propodus subchelate, triangular, strongly widening distally, anterior margin with several setae, palm as long as hind margin, transverse, strongly convex, margin crenate, with fine denticulations, with medial spines and lateral row of submarginal setules, palmar corner subrectangular with two spines; dactylus curved, as long as palm. *Gnathopod 2* (Fig. 15): coxa narrow, slightly tapering distally, width 0.5 × depth, apex rounded, ventral margin with two setae (one broken); basis straight, six thin setae at inner surface of anterior margin, 28 long setae forming circular patch anterodistally, posterior surface with some moderately long and long setae; merus, posterodistal lobe narrow and acute, setose; carpus strongly expanded, wider than propodus, anterior margin with ten setae (some delicately plumose), posterodistal lobe subacute, reaching palmar corner of propodus, distal margin oblique armed with a row of spines, posterior margin with moderately long setae; propodus shorter than carpus, subchelate, triangular, strongly widening distally, anterior margin with seven long setae regularly placed, palm shorter than hind margin, transverse, convex, margin crenate, with fine denticulations, with medial spines and lateral row of submarginal setules, palmar corner subrectangular with two spines; dactylus curved, slightly longer than palm. *Pereopod 3* (Fig. 16): coxa subrectangular, wider and deeper than coxa 2, ventral margin with some short setae; basis shorter than coxa, narrow, length 4.2 × width, anterior and posterior margins with some long setae; merus expanded distally, with two groups of setae anteriorly and three groups of setae posteriorly placed; carpus broad, length 1.2 × merus, posteriorly armed with long setae organized in 11 rows; propodus length 0.7 × carpus, with five rows of long setae anterodistally and 13 moderately long setae along posterior margin; dactylus thin, longer than propodus (1.4 × propodus). *Pereopod 4* (Fig. 16): coxa wider than deep, anterior margin slightly convex, extending distally, coxa the widest almost at the anteroventral corner, ventral margin armed with small setules, posteroventral lobe huge, blunt, (width to depth ratio of the lobe 1:0.7), posterior margin deeply excavated; basis long and narrow, length 4.7 × width, anterior and posterior margins with long, delicately plumose setae; merus weakly expanded, setose along anterior and posteror margins, a row of 12 long setae at anterodistal corner, a row of seven moderately long setae at posterodistal corner; carpus broad, length 0.8 × merus, 11 setae at anterodistal corner, posterior margin armed with *c.* 40 setae organized in ten rows; propodus narrow, length 0.8 × carpus, with seven rows of long setae along anterior margin and 9 moderately long setae along posterior margin (in five groups); dactylus stout, longer than propodus (1.5 × propodus). *Pereopod 5* (Fig. 17): coxa about as deep as coxa 4, bilobed, posterior lobe expanded ventrally, ventral margin straight with a few small setules, anterior lobe 0.6 × depth of posterior lobe; basis narrow, length 3.2 × width, long, delicately plumose setae at distal quarter of anterior margin (6), at posterior margin (5), and at the surface; merus as long as basis, with four groups of long, delicately plumose setae along anterior margin, four setae at anterodistal corner, four groups of moderately long setae posteriorly; carpus-dactylus broken off. *Pereopod 6* (Fig. 17): coxa bilobed but anterior lobe partly damaged, posterior lobe long, distal margin slightly convex; basis narrow, length 3.7 × width, posterior margin with 18 long and moderately long, delicately plumose setae, row of seven long setae at inner surface; merus length 0.7 × basis, five rows of setae anteriorly, four rows of setae posteriorly; carpus narrow, length 0.5 × merus, two rows of setae anteriorly and two rows of setae posteriorly; propodus narrow, length 1.9 × carpus, 14 setae along distal half of anterior margin and eight rows of setae posteriorly; dactylus broken. *Pereopod 7* (Fig. 17): coxa wider than deep, rounded posteriorly; basis ovate, length 1.5 × width, tapering distally, anterior margin strongly convex with short setae, proximally minute, triangular scales at the surface, posterior margin slightly oblique in distal half, smooth with two setae and a few setules proximally, posterodistal lobe absent; merus length 1.4 × basis with groups of setae both anteriorly and posteriorly (some setae broken); carpus-propodus broken off.

Pleon. *Pleonites* 1–2 (Fig. 13) with mid-dorsal, relatively long posteriorly directed teeth; pleonite 3 with short, upright tooth. *Epimera*: 1 and 3 evenly

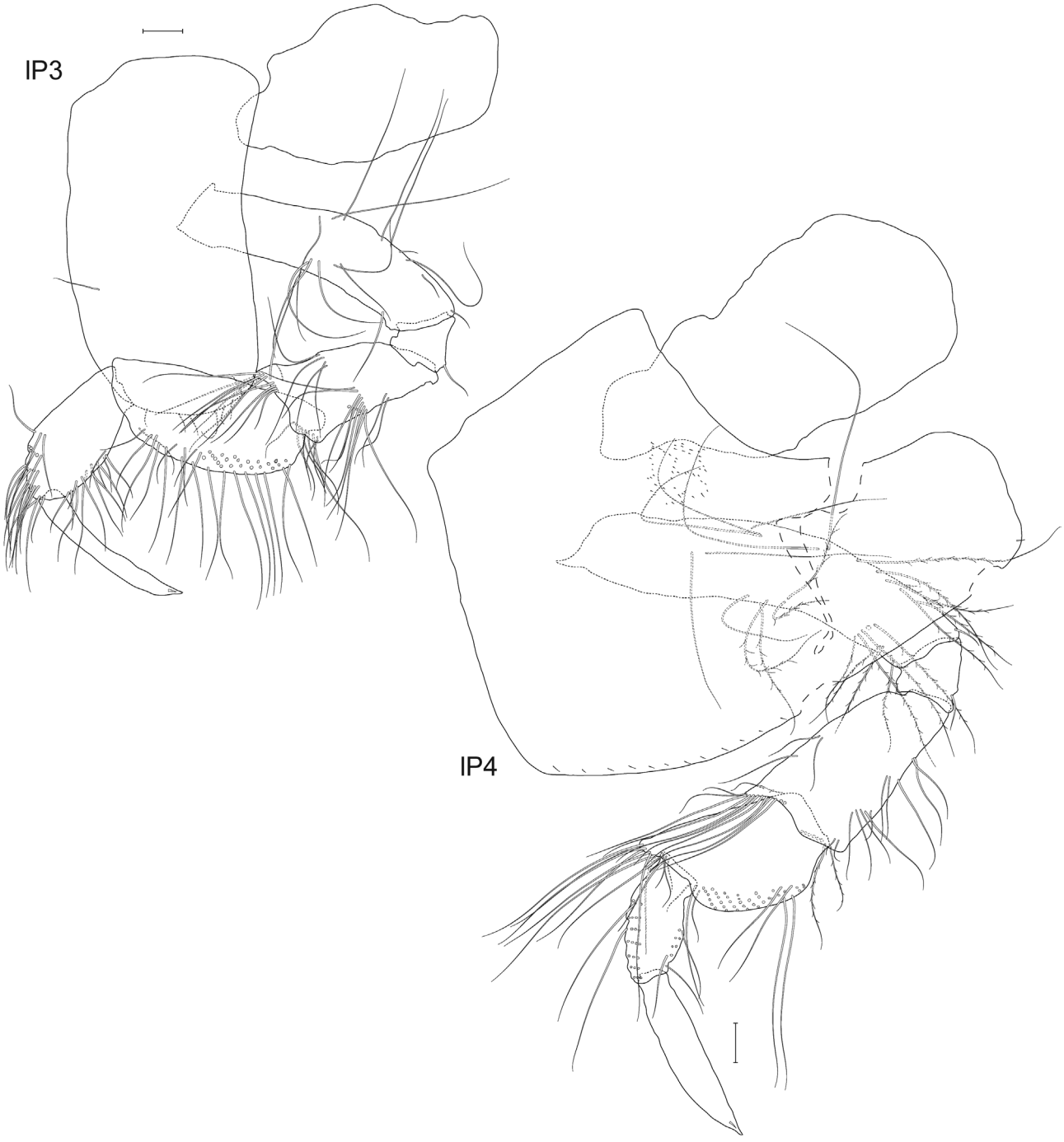

Figure 16. ***Oedicerina lesci*** **sp. nov.** Holotype female (SMF-56780, 10-7S_Oedi_2015_1): lP3, left pereopod 3; lP4, left pereopod 4. Scale bar = 0.1 mm, not all setae shown for clarity. The dashed line (long dashes) indicates the place where the appendage was damaged.

rounded, epimeron 2 posterior margin convex, posterodistal corner subquadrate. *Pleopods* [pleopod 2 (Fig. 18)]: powerful, peduncles and rami long.

Urosome. *Urosomite* 1 (Fig. 13) longest; urosomite 3 longer than 2, with short projection above telson.

Uropods (Fig. 18): *Uropod 1*: peduncle length 1.2 × inner ramus, margins with several short setae; inner ramus 1.3 × length of outer ramus, with small setae on both margins; outer ramus with setae on lateral margin only. *Uropod 2*: shorter than uropod 1, peduncle length 0.9 × inner ramus, with short setae on

Figure 17. ***Oedicerina lesci*** **sp. nov.** Holotype female (SMF-56780, 10-7S_Oedi_2015_1): lP5–lP7, left pereopod 5–7, respectively. Scale bar = 0.1 mm, not all setae shown for clarity. The dashed line (long dashes) indicates place where the appendage was damaged.

both margins; inner ramus 1.6 × length of outer ramus, with short setae on both margins; outer ramus with setae on lateral margin only. *Uropod 3*: peduncle short, peduncle length 0.3 × inner ramus; rami subequal, with traces of setae on lateral margins. *Telson*: (Fig. 18) short, length 1.5 × width, cleft 30%, lobes subacute,

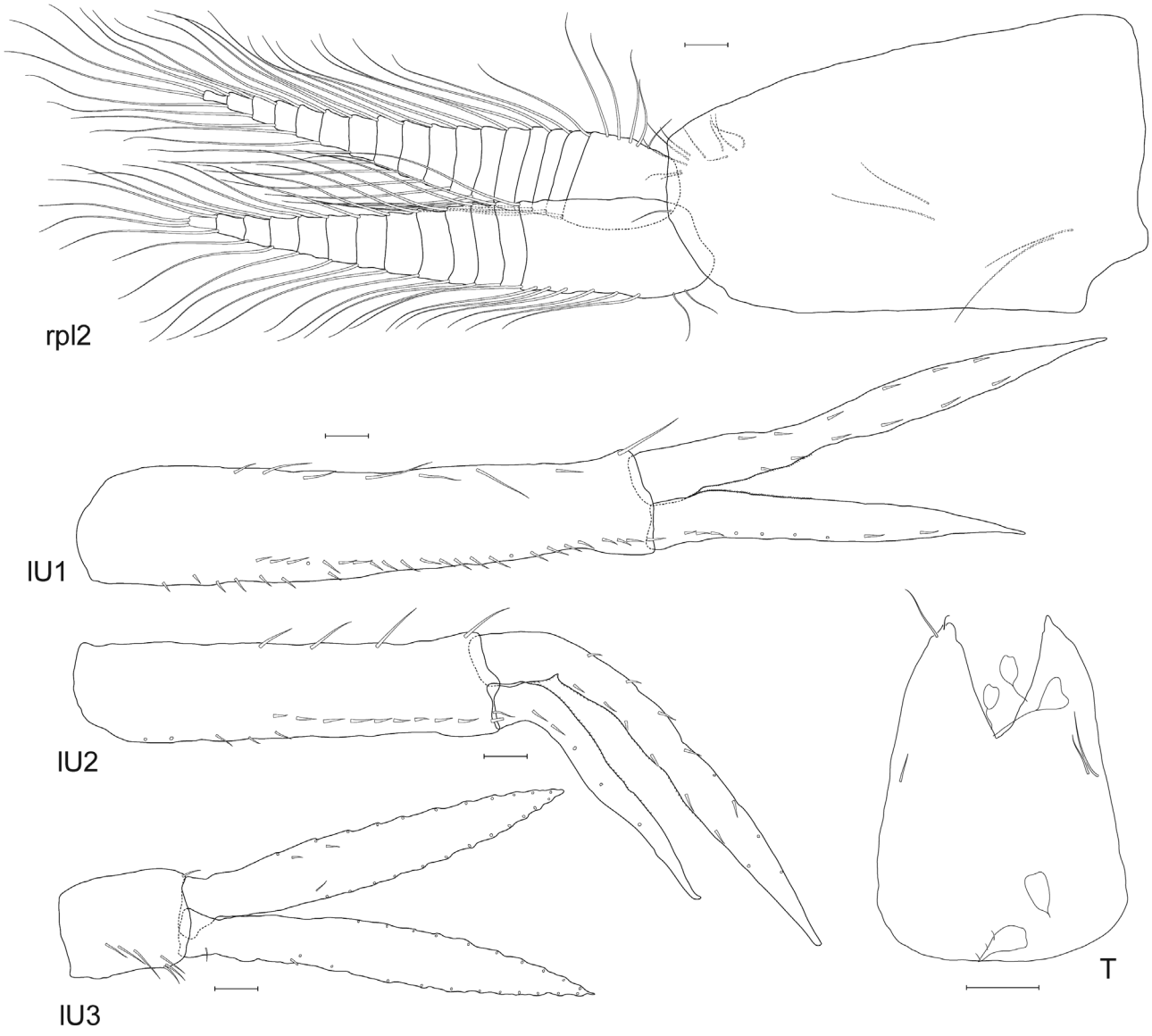

Figure 18. ***Oedicerina lesci*** **sp. nov.** Holotype female (SMF-56780, 10-7S_Oedi_2015_1): rpl2, right pleopod 2; lU1–U3, left uropod 1–3, respectively; T, telson. Scale bar = 0.1 mm, not all setae shown for clarity.

widely diverging, without subapical notches, with terminal setae, with a pair of dorsolateral setae, a few stalked protists (possibly ciliates) attached to the surface.

Intraspecific variation: The development of posterior teeth on pleonites 1–3 varies with size. In juveniles (3.1–7.0 mm) the teeth on pleonites 1–2 are weakly developed; however, the upright tooth on pleonite 3 is conspicuous. On the contrary, in larger individuals the teeth on pleonites 1–2 are distinct, whereas the upright tooth on pleonite 3 is weak. Urosomite 1 in some males is posteriorly slightly protruded forming a small hump (absent in females). Large individuals (both males and females) have urosomite 3 produced into a small subacute tooth over the telson.

Molecular identification: Following the definition given by Pleijel *et al.* (2008), the sequence of the holotype female of *O. lesci* (SMF-56780, GenBank accession number MW377941) is designed as a hologenophore of all obtained sequences. The sequences of the paratype and additional individuals of the species are deposited in GenBank with the following accession numbers: MN346311, MW377926, MW377928, MW377929, MW377933, MW377936,

MW377938, MW377940, MW377946. The species has received also a Barcode Index Number from BOLD: ADF5684 (dx.doi.org/10.5883/BOLD:ADF568).

Distribution: KKT area (Fig. 25), 4681–5419 m.

OEDICERINA CLAUDEI JAŻDŻEWSKA, SP. NOV.

(FIGS 19–23)

Zoobank registration: urn:lsid:zoobank.org:act:D1CB7EA5-FC38-406F-A101-BC5EBE7E1762.

Type material

Holotype: Juvenile, 4.5 mm, body remnants and two slides with appendages, SMF-56781, St. AKL-71-1-9, 46°05.037' N, 146°00.465' E-46°08.727' N, 146°00.227' E; 3307–3307 m, 10 July 2015, leg. Marina V. Malyutina.

The registered type material is deposited in the Senckenberg Museum (Frankfurt, Germany).

Type locality: Sea of Okhotsk, St. AKL-71-1-9, 46°05.037' N, 146°00.465' E-46°08.727' N, 146°00.227' E; 3307–3307 m.

Etymology: The species is named for Dr. Claude De Broyer, a great friend and one of the first author's scientific mentors and renowned specialist in amphipod taxonomy, diversity and ecology.

Description: Based on juvenile, 4.5 mm, St. AKL-71-1-9. *Head* (Fig. 19): longer than deep, longer than pereonites 1–4 combined; no eyes or ocular pigment visible; rostrum deflexed, the angle between head dorsal margin and rostrum margin almost 90 °, rostrum reaching the end of first article of peduncle of antenna 1; interantennal lobe indistinct. *Antenna 1* (Fig. 20): length ratios of peduncle articles 1–3 1:0.7:0.4, peduncle article 1 laterally acutely produced; flagellum 5-articulate, first article as long as article 3 of peduncle; accessory flagellum 1-articulate, minute, slender, length 0.2 × first flagellum article; peduncle and flagellum sparsely setose. *Antenna 2* (Fig. 20, considerably damaged): length of peduncle article 4 1.5 × article 5. *Upper lip* (labrum) (Fig. 20): wider than long, rounded apically, with fine setules laterally. *Mandible* (Fig. 20): incisor margins with five teeth; left lacinia mobilis four-cusped; right lacinia mobilis narrower slightly cuspidate; accessory spine rows with five serrate setae; molar columnar, strongly triturative, denticulate, with one associated seta; palp 3-articulate, article 1 short, article 2 1.1 × longer than article 3, with four posterodistal setae, article 3 slightly tapering distally, anterior margin with two setae, posterior margin with two setae, three setae at apex. *Lower lip* (Fig. 20): outer lobes broadly rounded, mandibular lobes narrow; inner lobes large, separate. *Maxilla 1* (Fig. 20): inner plate oval, with two distal setae; outer plate with eight acute setal-teeth (three with bifurcate tips); palp 2-articulate, longer than outer plate, slender, rounded apically, article 1 short, length 0.2 × article 2, article 2 with five or six apical/subapical setae and one long, lateral setae. *Maxilla 2* (Fig. 20): left—plates subequal in length, right—inner plate shorter than outer, inner plate width about 1.1 × outer, with setae and spines apically and subapically, fine setules along inner margin; outer plate rounded with apical spines and setae, outer margin with fine setules. *Maxilliped* (Fig. 21): inner plate subrectangular, reaching about 0.3 × basal article of palp, apical margin with six slender spines; outer plate slender and slightly curved, long, reaching 0.4 × length of palp article 2, apical and medial margins with setae and small spines; palp 4-articulate, strong; article 1 tapering distally; article 2 triangular, widest at 0.6 × length, setose medially; article 3 expanded mediodistally, slightly produced along article 4; article 4 strong, slightly curved; length ratios of articles 1–4 1:1.9:0.7:1.3.

Pereon. Pereonite 1 (Fig. 19) twice as long as pereonite 2, pereonite 3 longer than 2, pereonites 4–5 subequal in length, longer than pereonites 1–3, pereonites 6–7 of the same length, longer than all preceding segments. *Gnathopod 1* (Figs 19, 21): coxa subtriangular, anterodistal corner bluntly rounded, posterodistal corner rectangular, ventral margin naked, width to depth ratio 1:0.8; basis straight, slightly expanded distally, distal half of anterior margin with row of long setae, sparse setae on the surface; merus, posterodistal lobe subquadrate, moderately setose; carpus strongly expanded, anterior margin with five setae along distal half, posterior lobe subacute with setae along posterior and distal margins; propodus subchelate, triangular, strongly widening distally, anterior margin moderately setose, palm longer than hind margin, transverse, strongly convex, margin crenate, with fine denticulations, with medial spines and lateral row of submarginal setules, palmar corner subrectangular with one spine; dactylus curved, longer than palm. *Gnathopod 2* (Figs 19, 21): coxa narrow, slightly tapering distally, width 0.4 × depth, apex rounded, ventral margin naked; basis straight, 16 long setae forming circular patch anterodistally, single moderately long, delicately plumose seta at posterior margin; merus, posterodistal lobe rounded, moderately setose; carpus strongly expanded, wider than propodus, anterior margin with four setae (some delicately plumose), posterodistal lobe subacute, extending palmar corner of propodus, distal margin oblique armed with a row of spines, posterior margin with moderately long setae;

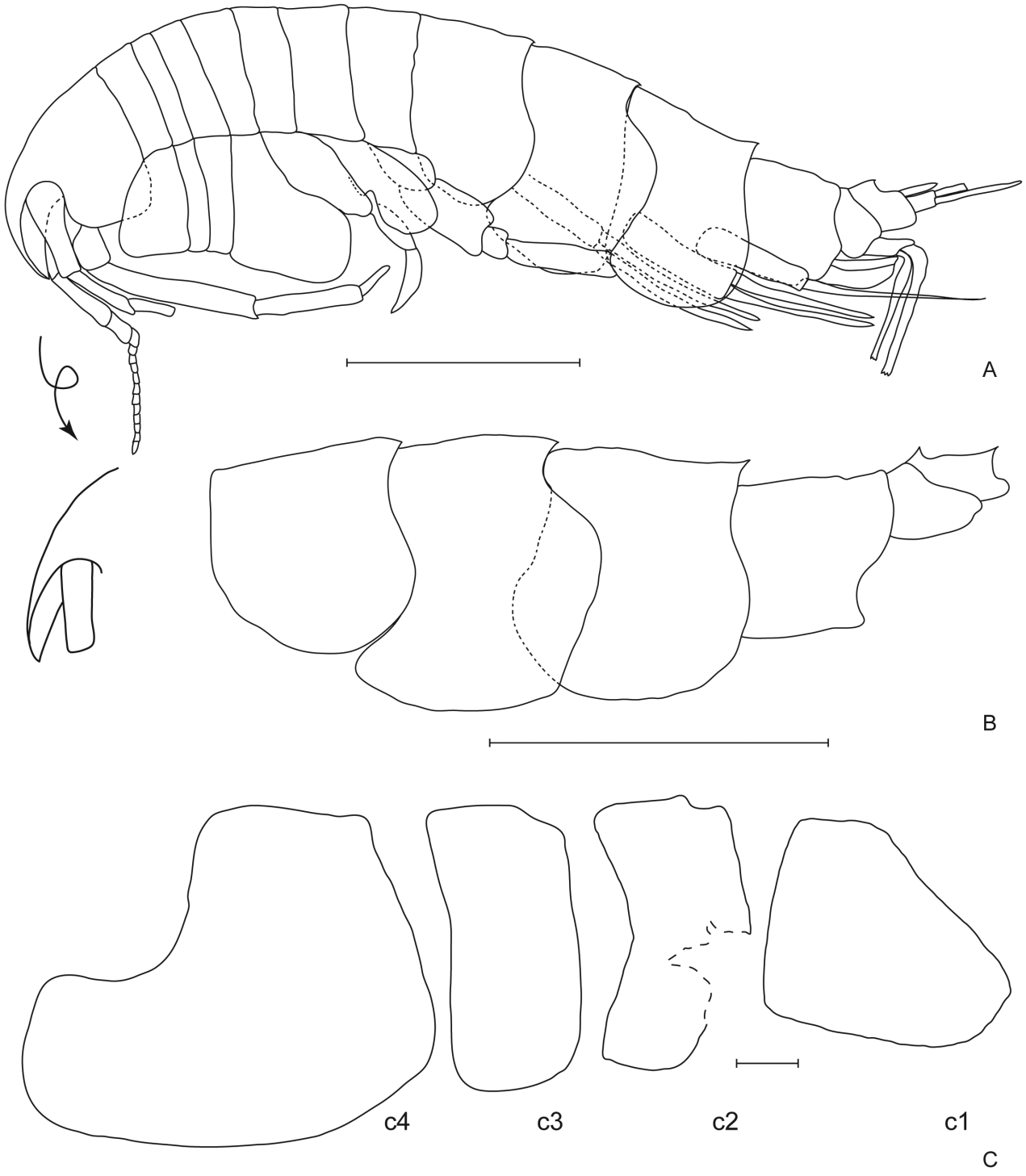

Figure 19. ***Oedicerina claudei*** **sp. nov.** Holotype juvenile (SMF-56781, 1-9S_Oedi_2015_1). A, habitus, arrow indicates close up of the rostrum. B, pleon and urosome. C, c1-4, right coxae 1–4. Scale bar A, B = 1 mm, C = 0.1 mm. The dashed line (long dashes) indicates the place where the appendage was damaged.

propodus shorter than carpus, subchelate, triangular, strongly widening distally, anterior margin with eight long setae regularly placed, palm shorter than hind margin, transverse, convex, margin crenate, with fine denticulations, with medial spines and lateral row of submarginal setules, palmar corner subrectangular

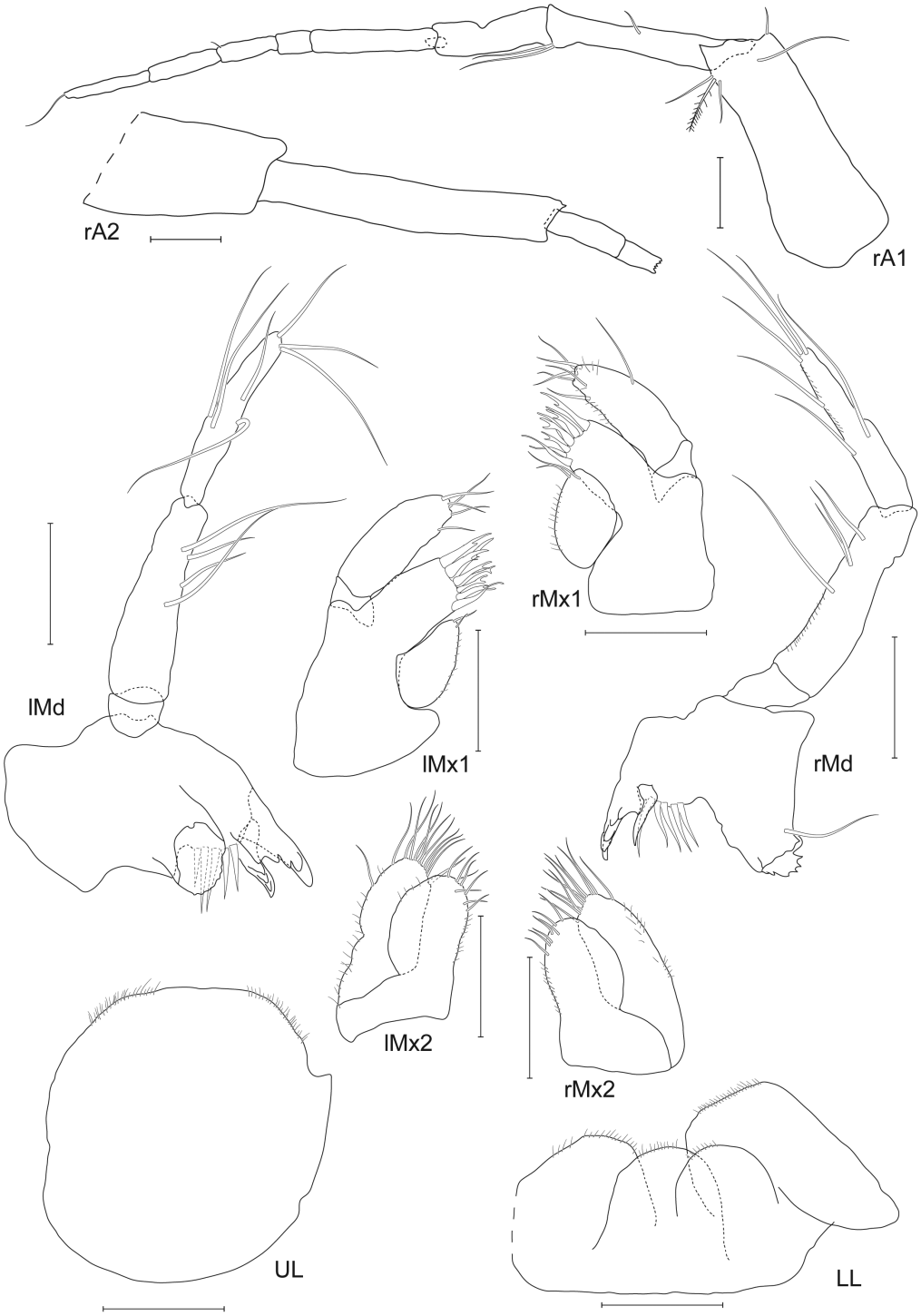

Figure 20. ***Oedicerina claudei*** **sp. nov.** Holotype juvenile (SMF-56781, 1-9S_Oedi_2015_1): rA1, right antenna 1; rA2, right antenna 2; lMx1, left maxilla 1; rMx1, right maxilla 1; lMd, left mandible; rMd, right mandible; UL, upper lip; lMx2, left maxilla 2; rMx2, right maxilla 2; LL, lower lip. Scale bar = 0.1 mm. The dashed line (long dashes) indicates the place where the appendage was damaged.

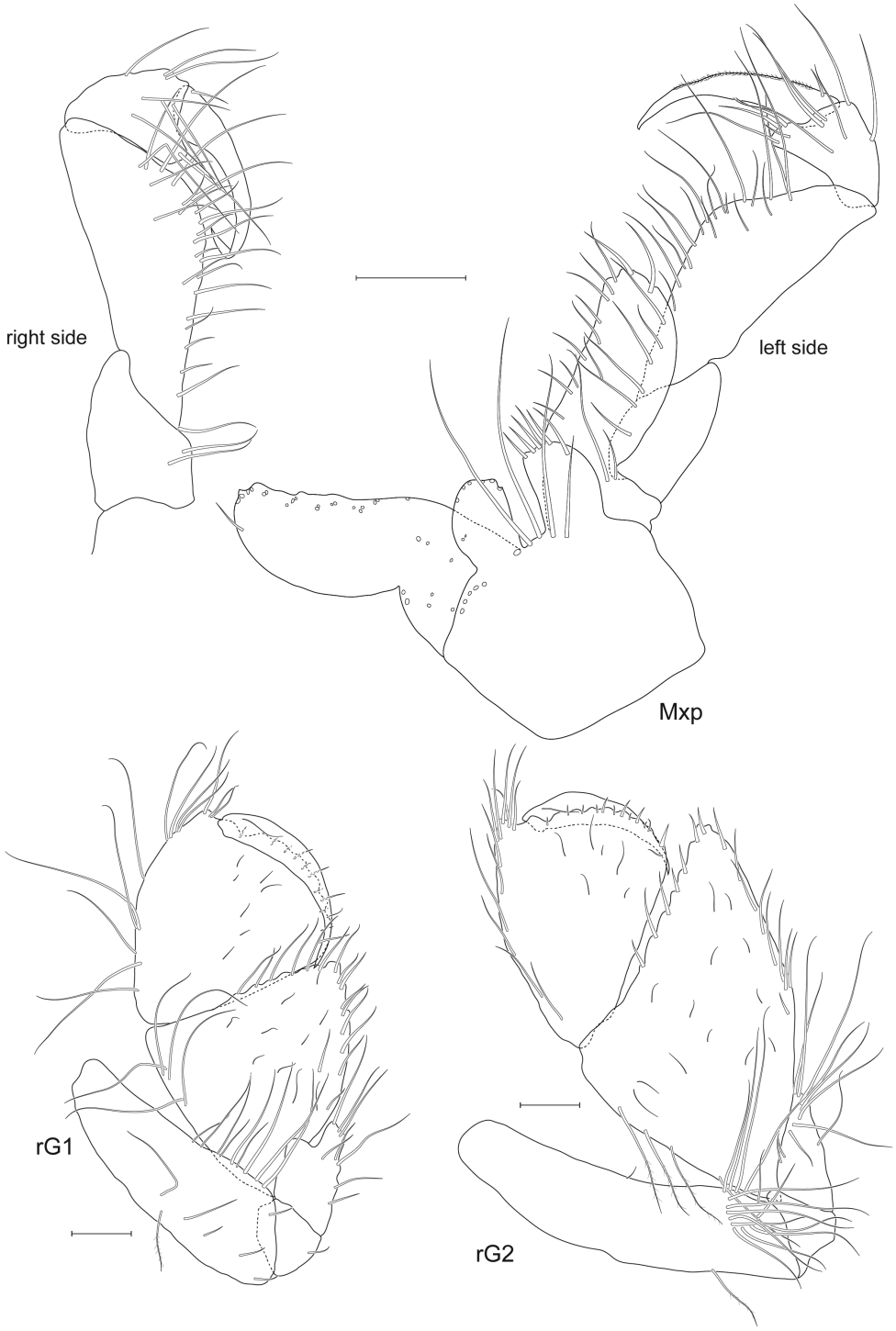

Figure 21. ***Oedicerina claudei*** **sp. nov.** Holotype juvenile (SMF-56781, 1-9S_Oedi_2015_1): Mxp, maxilliped; rG1, right gnathopod 1; rG2, right gnathopod 2. Scale bar = 0.1 mm, not all setae shown for clarity.

with one spine; dactylus curved, slightly longer than palm. *Pereopod 3* (Figs 19, 22): coxa subrectangular, wider and deeper than coxa 2, ventral margin naked; basis shorter than coxa, narrow, length 3.1 × width, anterior and posterior margins with some long, delicately plumose setae; merus expanded distally, one group of setae anterodistally and two groups of setae posteriorly; carpus broad, length 1.2 × merus,

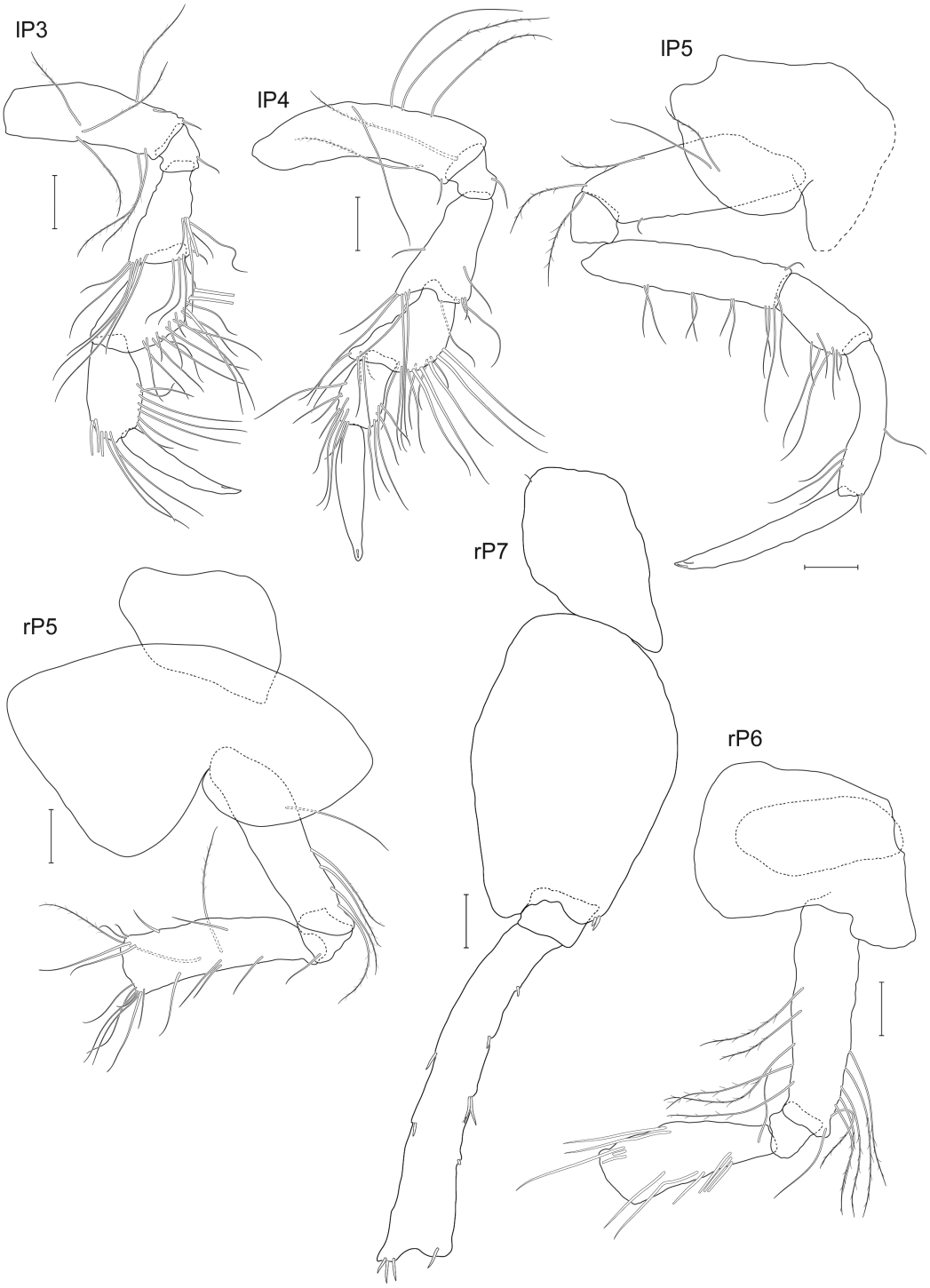

Figure 22. ***Oedicerina claudei*** **sp. nov.** Holotype juvenile (SMF-56781, 1-9S_Oedi_2015_1): lP3-lP5, left pereopod 3-5, respectively, rP5–rP7, right pereopod 5–7, respectively. Scale bar = 0.1 mm. The dashed line (long dashes) indicates the place where the appendage was damaged.

posteriorly armed with long setae; propodus length 0.8 × carpus, with six long setae anterodistally and seven long setae along posterior margin; dactylus stout, longer than propodus (1.2 × propodus). *Pereopod 4* (Figs 19, 22): coxa wider than deep, anterior margin strongly convex, extending distally, coxa the widest

almost at 2/3 of its depth, ventral margin naked, posteroventral lobe huge, blunt, (width to depth ratio of the lobe 1:0.9), posterior margin deeply excavated; basis long and narrow, length 3.5 × width, anterior margin with four long, delicately plumose setae, posterior margin with one long, delicately plumose setae, short seta at posterodistal corner; merus expanded, a few setae at anterior margin, one short seta at posterior margin, group of long setae at posterodistal corner; carpus expanded, length 0.8 × merus, five setae at anterodistal corner, posterior margin armed with 11 long and moderately long setae; propodus narrow, length 0.5 × carpus, moderately setose at anterior and posterior margins; dactylus stout, longer than propodus (1.9 × propodus). *Pereopod 5* (Fig. 22): right—coxa about as deep as coxa 4, bilobed, posterior lobe expanded ventrally, ventral margin straight, naked, anterior lobe 0.5 × depth of posterior lobe; basis narrow, length 4.1 × width, five long, delicately plumose setae at anterior margin; merus as long as basis, with three groups of moderately long plumose setae along anterior margin, seven setae at anterodistal corner, two setae at posterior margin and a group of four setae at posterodistal corner; carpus-dactylus broken off; left—coxa about as deep as coxa 4, bilobed, posterior lobe partially damaged; basis narrow, length 2.5 × width, two long, delicately plumose setae at anterior margin, two long setae at the surface (one delicately plumose); merus 1.1 × basis, with three groups of moderately long setae along anterior margin, four setae at anterodistal corner, two setae at posterior margin; carpus length 0.5 × merus, with five setae anterodistally; propodus length 1.6 × carpus length, with three setae anterodistally; dactylus stout, longer than propodus (1.2 × propodus length). *Pereopod 6* (Fig. 22): coxa bilobed but anterior lobe very small, posterior lobe long, distal margin slightly convex; basis narrow, length 3.9 × width, anterior margin with seven long, delicately plumose setae along distal half, posterior margin with five long, delicately plumose setae along distal half; merus length 0.7 × basis, three rows of setae anteriorly, two rows of setae posteriorly; carpus-dactylus broken off. *Pereopod 7* (Fig. 22): coxa wider than deep, rounded posteriorly; basis ovate, length 1.5 × width, widest in the mid-length, tapering distally, anterior margin strongly convex, two short spines at anterodistal corner, posterior margin slightly oblique in distal half, smooth, posterodistal lobe nearly as long as ischium; merus length 1.2 × basis with groups of setae both anteriorly and posteriorly (some setae broken); carpus-dactylus broken off.

Pleon. *Pleonite* 1 (Fig. 19) produced posteriorly, pleonites 2–3 with distinct mid-dorsal, posteriorly directed teeth. *Epimera*: 1 and 3 evenly rounded, epimeron 2 posterior margin convex, posterodistal corner subquadrate. *Pleopods* [pleopod 2 (Fig. 23)]: powerful, peduncles and rami long.

Urosome. *Urosomite* 1 (Fig. 19) longest; urosomite 3 longer than 2. *Uropods* (Fig. 23): *Uropod 1*: peduncle length 1.1 × inner ramus, margins with some short setae; inner ramus 1.4 × length of outer ramus, rami with sparse setae. *Uropod 2*: shorter than uropod 1, peduncle length 0.9 × inner ramus, with some short setae; inner ramus 1.2 × length of outer ramus, rami with sparse setae. *Uropod 3:* peduncle short, peduncle length 0.4 × inner ramus; inner ramus with short spines along distal half of lateral margins; outer ramus damaged. *Telson*: (Fig. 23) short, length 1.7 × width, cleft 40%, lobes subacute, widely diverging, notched subapically, tips unequal in size (inner longer than outer), single seta placed in the notch, single dorsolateral seta on the surface.

Sexual dimorphism: No sexual or size-dependent variation observed as the individual is unique.

Molecular identification: Following the definition given by Pleijel *et al.* (2008), the sequence of the holotype juvenile of *O. claudei* (SMF-56781, GenBank accession number MW377945) is designed as a hologenophore of all obtained sequences. The species has received also a Barcode Index Number from BOLD: AEA4699 (dx.doi.org/10.5883/BOLD:AEA4699).

Distribution: Sea of Okhotsk (Fig. 25), 3307 m.

Molecular investigation

Each of the morphologically recognized species received a unique Barcode Index Number. Across all species, the intraspecific diversity calculated on haplotypes is low, ranging from 0.002 (*O. lesci*) to 0.005 (*O. henrici*) for both K2P and *p*-distance. Each of the species is represented by three haplotypes (Table 2; Fig. 24B). An exception is *O. claudei*, as only one individual of this taxon was collected. The distances between the studied taxa varies from 0.059 to 0.238 of *p*-distance and from 0.061 to 0.289 of K2P (Table 3). The lowest interspecies distances are noted between *O. lesci* and *O. ingolfi*, irrespective of the measures applied. The highest values are observed for *O. henrici* and *O. claudei* for both measures and for *O. henrici* and *O. ingolfi* for *p*-distance only (Fig. 24A).

The haplotype networks show a star-like topology (Fig. 24B). In *O. lesci*, the central, ancestral and dominant haplotype is present at five stations including the stations situated on both sides of the KKT. In *O. henrici* and *O. teresae*, the central, ancestral haplotypes are missing.

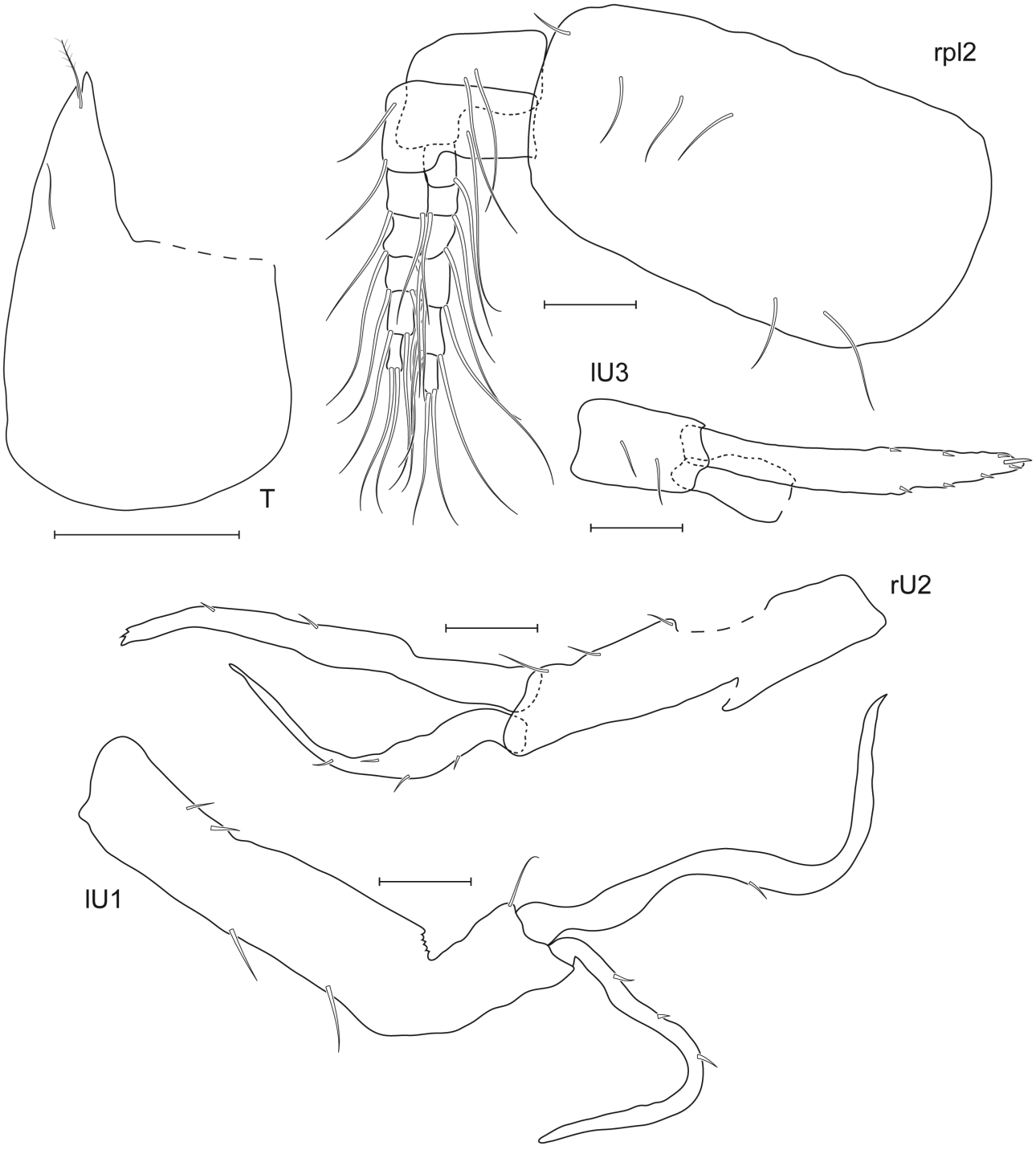

Figure 23. ***Oedicerina claudei*** **sp. nov.** Holotype juvenile (SMF-56781, 1-9S_Oedi_2015_1): rpl2, right pleopod 2; lU1, left uropod 1; rU2, right uropod 2; lU3, left uropod 3; T, telson. Scale bar = 0.1 mm. The dashed line (long dashes) indicates the place where the appendage was damaged.

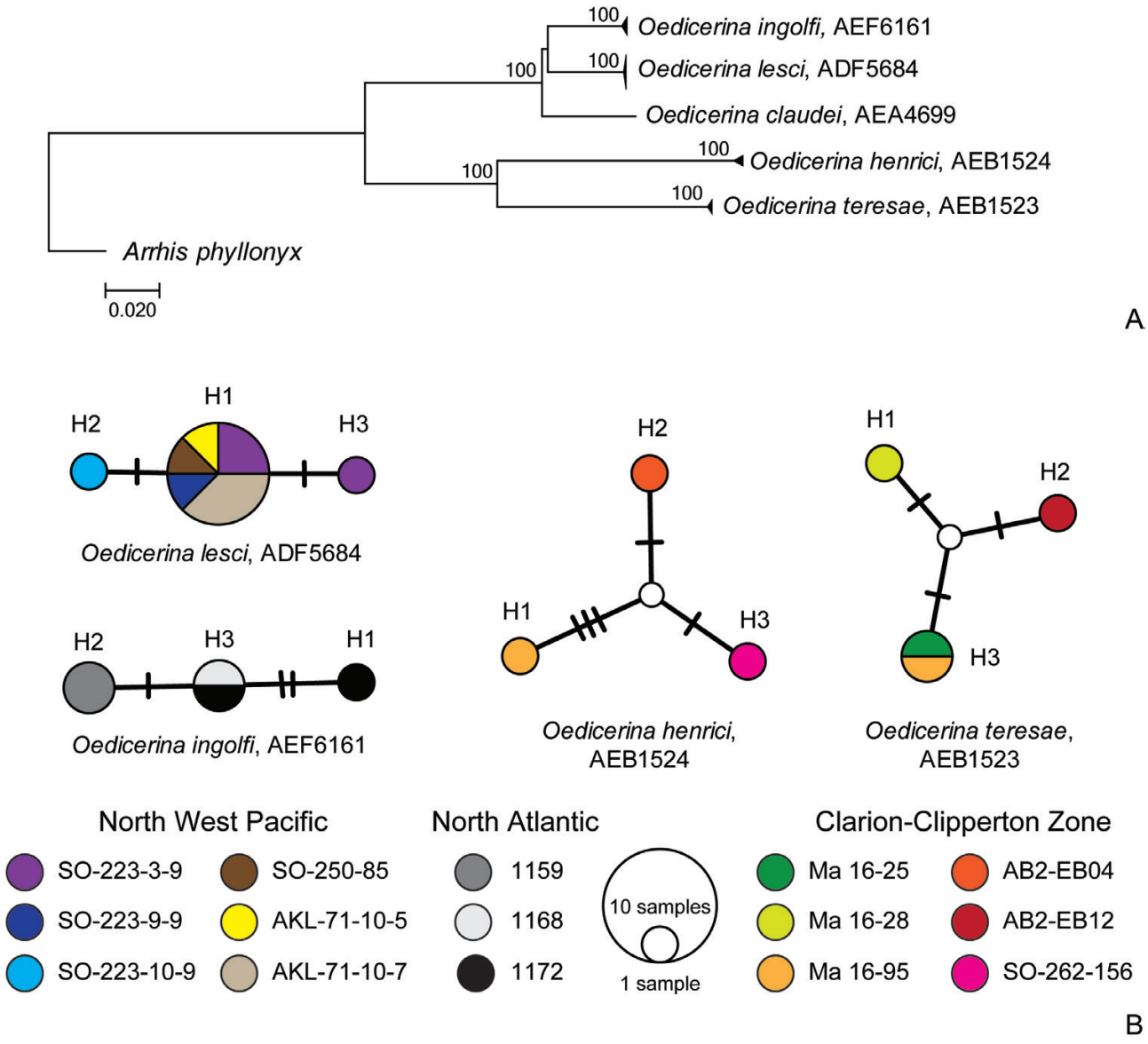

Figure 24. A, neighbour-joining tree of the *COI* sequences of the four newly described species and *O. ingolfi* collected in the North Atlantic. Codes represent the Barcode Index Numbers (BINs) ascribed by the Barcode of Life Data System (BOLD). The distances were calculated using the *P*-distance method. Triangles indicate the relative number of individuals studied (height) and sequence divergence (width). The numbers in front of the nodes indicate bootstrap support (1000 replicates, only values higher than 50% are presented). Note that this tree does not represent a reconstruction of evolutionary history of the presented taxa. B, median joining network of the identified haplotypes. Each line represents a mutation between sequences. Colours denote sampling stations.

DISCUSSION

MORPHOLOGICAL DIFFERENCES BETWEEN *OEDICERINA* SPECIES

With the description of four new species, the number of known *Oedicerina* species is almost doubled. Coleman & Thurston (2014) indicated high similarity of the species within this genus because only a few characters were used for species recognition (mainly ornamentation of pleonites and urosomites). This was noted also in the present study; our new data document that there are only minute differences in the mouthparts observed between species, i.e. in the setation of the mandibular palp, the shape of article 3 of the maxilliped palp (Table 4). In *O. claudei* and *O. teresae*, the number of setal teeth on the inner plate of maxilla 1 was eight (nine in all other species). However, this difference may derive from the fact that

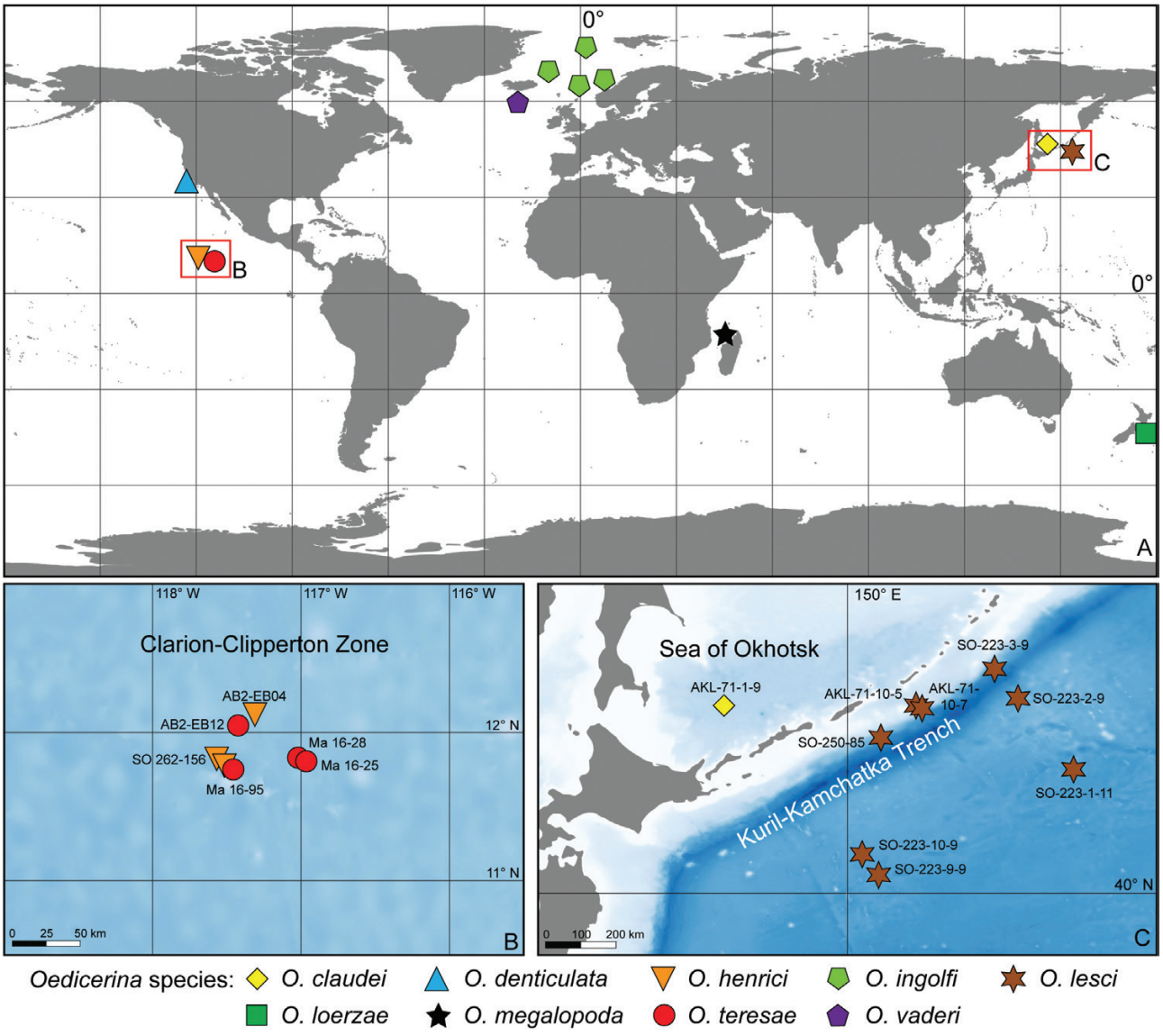

Figure 25. Geographic distribution of the *Oedicerina* species. A, world distribution of all known species. B, the CCZ with the sampling stations shown where ***O. henrici* sp. nov.** and ***O. teresae* sp. nov.** were collected. C, KKT area with the sampling stations shown where ***O. lesci* sp. nov.** and ***O. claudei* sp. nov.** were collected. Station codes as in Table 1.

in both cases the studied individuals were not fully developed adults. Nevertheless, a number of characters differentiating species were observed. Apart from the already mentioned differences in the mouthparts, further differences are observed in the shape of the rostrum and its curvature, in the shape and setation of coxae 1–4, the length of dactylus of both gnathopods and pereopods 3–4, the shape of the basis of pereopod 7 as well as the shape of the lateral lobes of the telson. Additionally, some differences were observed in the ornamentation (size and shape of dorsal teeth) of pereon segment 7, the pleonites and urosomite 1.

Of the four species described here, two i.e. *O. henrici* and *O. claudei*, belong to taxa with a strongly deflexed rostrum. They share this feature with *O. denticulata*, *O. megalopoda* and *O. vaderi*. From all these species *O. henrici* can be separated by the first coxal plate that is distinctly wider than deep whereas in the remaining species both dimensions of coxa 1 are similar. Additionally, *O. henrici* differs from *O. megalopoda* in the shape of maxilliped article 3 that is strongly produced in the latter and unproduced in the former. The differences are also observed in the shape of the basis of pereopod 7. In both *O. henrici* and in *O. vaderi*

Table 2. Barcode Index Numbers (BINs), number of sequences and haplotypes as well as genetic distances for *COI* haplotypes calculated using uncorrected *p*-distance and Kimura 2-parameter (K2P) for the newly described species and *O. ingolfi*

	BIN	No. of seq.	No. of haplotypes	*p*-distance	K2P
O. lesci	ADF5684	10	3	0.002	0.002
O. claudei	AEA4699	1	1	–	–
O. teresae	AEB1523	4	3	0.003	0.003
O. henrici	AEB1524	3	3	0.005	0.005
O. ingolfi	AEF6161	5	3	0.003	0.003

Table 3. *COI* mean interspecies distances based on haplotypes between studied species (*p*-distance lower left, K2P upper right). The lowest values are indicated in bold, the highest values are shown in italics

	O. lesci	*O. claudei*	*O. teresae*	*O. henrici*	*O. ingolfi*
O. lesci		0.070	0.274	0.285	**0.061**
O. claudei	0.066		0.270	*0.289*	0.065
O. teresae	0.228	0.225		0.196	0.266
O. henrici	0.236	*0.238*	0.170		0.288
O. ingolfi	**0.059**	0.062	0.223	*0.238*	

it is slightly tapering distally; however, the posterior margin is slightly crenulated in the newly described species, while it is smooth in the latter. In *O. claudei* and in *O. denticulata* the shape of the basis is more ovate, but the first species possesses a posterodistal lobe nearly as long as the ischium, which is absent in *O. denticulata*. *O. henrici* is characterized by the presence of dorsal teeth on pereonite 7 and pleonites 1–3, that are absent in *O. vaderi*. In *O. denticulata* they are developed on pleonites 2–3, while in *O. claudei* a small tooth is observed on pleonite 3 only.

The group of the remaining four species shares the curved but not strongly deflexed rostrum. Within them only *O. teresae* possesses dorsal teeth on pereonite 7 and pleonites 1–3. Both *O. ingolfi* and *O. lesci* have a smooth dorsal surface in pereonite 7 and pleonites 1–3 each possess a single tooth. In *O. loerzae* only pleonites 1 and 2 are toothed. *O. teresae* differs from the other species also by the shape of coxa 1 that has the anteroventral corner subacute whereas it is bluntly rounded in the remaining species. *O. lesci* and *O. ingolfi* share many morphological characters. They can be separated by the shape of coxa 4 that is the widest at 2/3 of its length in *O. lesci* whereas in the other species it is widest close to the anteroventral corner. Additionally, the shape of the basis of pereopod 7 allows to distinguish the two species. It is posteriorly weakly sinuous in *O. ingolfi*, whereas in *O. lesci* it is straight. These two species differ also in the setation of coxal plates 1–3 which is distinctly denser in *O. ingolfi*.

Molecular study and biogeographical remarks

The studied taxa presented a low level of intraspecific variability, as three haplotypes were recorded for each of the studied species. It has to be stressed that in the case of *O. henrici* and *O. teresae*, a low number of individuals was collected and the sampling covered only a small part of the potential species range. Further studies are required to assess more precisely the level of intraspecific variation in these taxa.

By contrast, *O. lesci* was represented by almost 30 individuals collected on both sides of the KKT (Fig. 25C). This distribution was confirmed by molecular results that distinguished three closely related haplotypes. In the same area, a comparatively low intraspecific diversity was observed among representatives of two families grouping moderately mobile Isopoda (Bober *et al.*, 2018b, 2019). In *O. lesci* the dominant haplotype appeared to be shared by individuals coming from stations situated on both sides of the trench as far as 700 km from each other (Fig. 24B). A recent molecular study of Amphipoda from the abyss adjacent to the KKT has also confirmed that this physiographic feature does not constitute a complete barrier for the gene flow of some molecularly

Table 4. Morphological comparison of new species of *Oedicerina* including known species with information about their geographic and bathymetric distribution

Species/ character	*Oedicerina claudei* sp. nov.	*Oedicerina denticulata* Hendrycks & Conlan, 2003	*Oedicerina henrici* sp. nov.	*Oedicerina ingolfi* Stephensen, 1931
Head rostrum (shape)	Moderately deflexed, the angle between the dorsal head margin and rostrum margin a little more than 90 °	Strongly deflexed, the angle between the dorsal head margin and rostrum margin *c.* 90 °	Strongly deflexed, the angle between the dorsal head margin and rostrum margin 90 ° or less	Not deflexed, wide angle between the head dorsal margin and rostrum margin
Head rostrum (length)	As long as 1st article of peduncle A1	As long as 1st article of peduncle A1	As long as 1st article of peduncle A1	2/3 length of 1st article of peduncle A1
Md palp	2nd article, 4 setae; 3rd article, 2 medial, 2–3 apical setae	2nd article, *c.* 11 setae; 3rd article, 6 medial, 3 apical setae	2nd article, *c.* 10 setae; 3rd article, row of setae (30)	2nd article, *c.* 12 setae; 3rd article, 9 medial, 3 apical setae
Mxp	3rd palp article slightly produced along 4th	3rd palp article slightly produced along 4th	3rd palp article not produced along 4th	3rd palp article slightly produced along 4th
Coxa 1	Subtriangular, anterodistal corner bluntly rounded, ventral margin naked	Subtriangular, anterodistal corner bluntly rounded, ventral margin setose (curled setae)	Subtriangular, distinctly produced anteriorly, anterodistal corner narrowly rounded, ventral margin naked	Subtriangular, anterodistal corner bluntly rounded, ventral margin densely setose (long setae)
C1 width/depth	1:0.8	1:0.9	1:0.7	1:0.9–1
G1 dactylus	Longer than palm	As long as palm	Longer than palm	Just longer than palm
Coxa 2	Ventral margin naked	Ventral margin setose (curled setae)	Ventral margin naked	Ventral margin densely setose
G2 dactylus	Longer than palm	Slightly shorter than palm	Longer than palm	As long as palm
Coxa 3	Ventral margin naked	Ventral margin setose	Ventral margin naked	Ventral margin setose
P3 dactylus	Longer than propodus (1:1.3)	Longer than propodus (1:1.2)	Shorter than propodus (1:0.7)	Longer than propodus (1:1.2)
C4 shape	Front margin strongy extending distally, coxa the widest at two-thirds of length	Front margin almost straight	Front margin almost straight	Front margin slightly extending distally, coxa the widest at two-thirds of length
C4 lobe width/ depth	1:0.9	1:0.7	1:0.5	1:0.8–1
P4 dactylus	Longer than propodus (1:1.8)	Longer than propodus (1:1.4)	Unknown	Longer than propodus (1:1.2–1.3)
Basis P7	Posterior margin convex, the widest in the middle of the length, smooth, with posterodistal lobe nearly as long as ischium, width:length = 1:1.4	Ovate, slightly tapering distally, posterior margin with long plumose setae, width:length = 1:1.4	Slightly tapering distally, posterior margin straight, crenutaled, naked, width:length = 1:1.6	Posterior margin weakly sinuous, smooth, sparse long plumose setae, some short setae, width:length = 1:1.5
Pereonites teeth	Smooth	Smooth	Pereonite 7 posteriorly directed tooth	Smooth
Pleonite 1	Smooth	Smooth	Posteriorly directed tooth	Posteriorly directed tooth
Pleonite 2	Smooth	Posteriorly directed tooth	Posteriorly directed tooth	Posteriorly directed tooth
Pleonite 3	Small, posteriorly directed tooth	Short upright process	Small, posteriorly directed tooth	Small, upright tooth

***Oedicerina lesci* sp. nov.**	***Oedicerina loerzae*** Coleman & Thurston, 2014	***Oedicerina megalopoda*** Ledoyer, 1986	***Oedicerina teresae* sp. nov.**	***Oedicerina vaderi*** Coleman & Thurston, 2014
Not deflexed, wide angle between the head dorsal margin and rostrum margin	Not deflexed, wide angle between the head dorsal margin and rostrum margin	Strongly deflexed, the angle between the dorsal head margin and rostrum margin *c*. 90 °	Not deflexed, wide angle between the head dorsal margin and rostrum margin	Strongly deflexed, the angle betweenthe dorsal head margin and rostrum margin *c*. 90 °
Two-thirds length of 1st article of peduncle a1	Two-thirds length of 1st article of peduncle A1	Shorter than 1st article of peduncle A1	Two-thirds length of 1st article of peduncle A1	Shorter than 1st article of peduncle A1
2nd article, *c*. 18 setae; 3rd article, 10 medial, 2–3 apical setae	2nd article, *c*. 15 setae; 3rd article, row of setae (20)	2nd article, *c*. 10 setae; 3rd article, row of setae	2nd article, 7 setae; 3rd article, 11 medial, 2–3 apical setae	2nd article, *c*. 15 setae; 3rd article, row of setae (23)
3rd palp article distinctly produced along 4th	3rd palp article slightly produced along 4th	3rd palp article strongly produced along 4th	3rd palp article not produced along 4th	3rd palp article not produced along 4th
Subtriangular, anterodistal corner bluntly rounded, ventral margin setose (moderately long setae)	Subtriangular, anterodistal corner bluntly rounded, ventral margin sparcely setose (short setae)	Subtriangular, anterodistal corner bluntly rounded, ventral margin setose (setae broken)	Subtriangular, anterodistal corner “subacute”, ventral margin with single seta anteriorly placed	Subtriangular, anterodistal corner bluntly rounded, ventral margin sparcely setose (short setae)
1:0.9	1:1	1:1	1:1	1:0.8
As long as palm	Just longer than palm, palmar corner not well defined	As long as palm, palmar corner not well defined	Distinctly longer than palm	As long as palm
Ventral margin weakly setose	Ventral margin with a few short setae	Ventral margin setose (setae broken)	Ventral margin naked	Ventral margin with single seta
Just longer than palm	Just longer than palm, palm straight	As long as palm, palm straight	Just longer than palm	As long as palm
Ventral margin sparcely setose	Ventral margin with a few short setae	Ventral margin setose (setae broken)	Ventral margin naked	Ventral margin sparcely setose
Longer than propodus (1:1.4)	Longer than propodus (1:1.6)	Unknown	As long as propodus	As long as propodus
Front margin slightly extending distally, coxa the widest almost at the anteroventral corner	Front margin slightly extending distally, coxa the widest at 2/3 of length	Front margin slightly extending distally, coxa the widest at 2/3 of length	Front margin strongly extending distally, coxa the widest at two-thirds of length	Front margin strongly extending distally, coxa the widest at two-thirds of length
1:0.7	1:0.6	1:0.7	1:0.7	1:0.7
Longer than propodus (1:1.5)	Longer than propodus (1:1.8)	Longer than propodus (1:1.8)	Unknown	Longer than propodus (1:1.5)
Slightly tapering distally, posterior margin straight, smooth, sparse short setae anteriorly, width:length = 1:1.4	Posterior margin straight, slightly tapering distally, smooth, a few short setae, posterodistal lobe nearly as long as ischium, width:length = 1:1.3	Unknown	Basis ovate, the widest in the middle of the length, posterior margin denticulate, naked, width:length = 1.1:5	Slightly tapering distally, posterior margin straight, smooth, naked, width:length = 1:1.5
Smooth	Smooth	Unknown	Pereonite 7 posteriorly directed tooth	Smooth
Small, posteriorly directed tooth	Posteriorly directed tooth	Unknown	Posteriorly directed tooth	Smooth
Posteriorly directed tooth	Posteriorly directed tooth	Unknown	Posteriorly directed tooth	Smooth
Small, upright tooth	Smooth	Unknown	Large, posteriorly directed tooth	Smooth

Table 4. Continued

Species/ character	*Oedicerina claudei* sp. nov.	*Oedicerina denticulata* Hendrycks & Conlan, 2003	*Oedicerina henrici* sp. nov.	*Oedicerina ingolfi* Stephensen, 1931
Urosomite 1	Smooth	Smooth	Middle sized, upright tooth, small boss in the mid length of urosomite	Smooth
Telson	Lobes notched subapically, tips unequal in size (inner longer than outer)	Lobes notched subapically, tips unequal in size (inner longer than outer)	Lobes notched subapically	Lobes without notches
Distribution	NW Pacific, Sea of Okhotsk	NE Pacific, California	NE Pacific, CCZ	N Atlantic, north of Iceland
Depth range (m)	3307	4050	4111–4359	1802–3200

identified benthic species (Jażdżewska & Mamos, 2019). The dispersal of benthic amphipods that are brooders depends only on adults whose swimming abilities differ between species. The identification of the taxa in the above cited research was preliminary thereby prohibiting a final conclusion regarding the influence of lifestyle on the genetic connectivity of these species. Nevertheless, within the group of ten molecularly defined taxonomic units that appeared to be present on both sides of the KKT as many as nine belonged to the taxa of higher mobility—the Eusiridae, Lysianassoidea, Pardaliscidae, Synopiidae and Vemanidae. However, one species of that group was identified as a representative of the family

A KEY TO ALL KNOWN SPECIES OF *OEDICERINA*:

1a. Rostrum strongly deflexed, the angle between the head dorsal margin and rostrum margin *c.* 90 ° (Fig. 1A) 2
1b. Rostrum curved but not strongly deflexed, the angle between the head dorsal margin and rostrum margin distinctly larger than 90 ° (Fig. 1B) 5
2a. Coxa 1 distinctly wider than deep (width length ratio 1:0.7), anterodistal corner narrowly rounded ..... *O. henrici*
2b. Coxa 1 slightly wider than deep or as wide as long (width length ratio 1:0.8–1.0), anterodistal corner broad, bluntly rounded.....3
3a. Gnathopod 2 palm straight, maxilliped palp article 3 strongly produced along article 4 ..... *O. megalopoda*
3b. Gnathopod 2 palm strongly convex, maxilliped palp article 3 slightly or not produced along article 4 4
4a. Coxae 1–3 setose (long curled setae), pereopod 7 posterior margin of basis with long plumose setae, posterodistal lobe absent ..... *O. denticulata*
4b. Coxa 1–3 sparsely setose (short setae), pereopod 7 posterior margin of basis naked, posterodistal lobe absent ..... *O. vaderi*
4c. Coxae 1–3 naked, pereopod 7 posterior margin of basis naked, posterodistal lobe present, nearly as long as ischium ..... *O. claudei*
5a. Pereonite 7 with posteriorly directed tooth, gnathopod 1 dactylus distinctly longer than palm ... *O. teresae*
5b. All pereonites smooth posteriorly, gnathopod 1 dactylus as long as palm or only minutely longer than palm 6
6a. Pleonite 3 smooth posteriorly, pereopod 7 posterodistal lobe present, almost as long as ischium . *O. loerzae*
6b. Pleonite 3 with small upright tooth, pereopod 7 posterodistal lobe absent..... 7
7a. Coxa 4 anterior margin slightly expanding distally, coxa the widest almost at the anterodistal corner, maxilliped palp article 3 distinctly produced along article 4 ..... *O. lesci*
7b. Coxa 4 anterior margin slightly expanding distally, coxa the widest at 2/3 of its length, maxilliped palp article 3 slightly produced along article 4 ..... O. ingolfi

***Oedicerina lesci* sp. nov.**	***Oedicerina loerzae*** Coleman & Thurston, 2014	***Oedicerina megalopoda*** Ledoyer, 1986	***Oedicerina teresae* sp. nov.**	***Oedicerina vaderi*** Coleman & Thurston, 2014
Smooth	Smooth	Unknown	Large, upright tooth	Low rounded boss
Lobes without notches	Lobes without notches	Unknown	Lobes notched subapically, tips unequal in size (inner slightly shorter than outer)	Lobes notched subapically, tips unequal in size (inner longer than outer)
NW Pacific, abyss adjacent to the KKT	SW Pacific, Chatham Rise	Indian Ocean, off Madagascar	NE Pacific, CCZ	N Atlantic, south of Iceland
4681–5419	478–530	200–500	4101–4359	2636–2646

Phoxocephalidae grouping benthic dwellers (Brix *et al.*, 2018b; Jażdżewska & Mamos, 2019). These results support previous assumptions that abyssal species display wide geographic ranges and that underwater physical barriers have no or only moderate influence on genetic connectivity (Zardus *et al.*, 2006; Brix *et al.*, 2011, 2015; Etter *et al.*, 2011). A study of the isopod family Haploniscidae in the NW Pacific based exclusively on morphological identification also revealed some species occurring on both sides of the KKT (Johanssen *et al.*, 2019). However, recent molecular studies based on isopods indicate that the lifestyle of the studied group may influence the geographic range of species (Bober *et al.*, 2018a; Brix *et al.*, 2018a, 2020; Riehl *et al.*, 2018). Good swimming abilities may promote genetic exchange between populations living across the trench, as observed for *Rhachotropis saskia* Lörz & Jażdżewska, 2018 (Lörz *et al.*, 2018). The family Oedicerotidae, to which the newly described species belong, includes benthic infaunal taxa regarded as permanent burrowers (De Broyer *et al.*, 2003; Brix *et al.*, 2018b). As a result they are considered to be moderately mobile and their population connectivity seems to be restricted leading to higher genetic structure. However, an example of interesting behaviour potentially explaining higher than expected gene exchange of this moderately mobile group of amphipods was noted in some shallow-water oedicerotids as they were observed to migrate into the water column for reproduction (Brix *et al.*, 2018b). Nothing is known about the mating behaviour of deep-sea species from this family; however, Hendrycks & Conlan (2003) reported *O. denticulata* from samples collected at least 50 m above the seafloor, supporting the assumption that despite having an ability to dig in the sediment, at least some of the species in this genus may also occur in the water column. Based on our results *O. lesci* has its occurrence restricted to abyssal depths (4681–5419 m), while the KKT extends down to *c.* 9500 m depth (Dreutter *et al.*, 2020). A study of the bathymetric distribution of 28 MOTUs of Amphipoda from the KKT and adjacent abyssal plain revealed only four MOTUs being present both in the abyss and the hadal zone (Jażdżewska & Mamos, 2019). The identification of the collection coming from the deepest stations in the KKT has not been finished yet, however, to date there is no evidence of the presence of *O. lesci* at hadal depths (Jażdżewska A, pers. obs.). Consequently, it may be assumed that the dispersal of this species along and across the trench depends on its swimming over the bottom, possibly also taking advantage of the near-bottom currents flowing in that area (Mitsuzawa & Holloway, 1998) instead of crawling on the sediment surface.

The species of the genus *Oedicerina* were found in all three oceans in both the Northern and Southern Hemispheres (Fig. 25A) (Stephensen, 1931; Ledoyer, 1986; Hendrycks & Conlan, 2003; Coleman & Thurston, 2014). Two species, *O. ingolfi* and *O. vaderi*, occur in the North Atlantic, *O. megalopoda* in the Indian Ocean and the remaining six species in the Pacific. *O. loerzae* was described from the bathyal of the Chatham Rise and it constitutes the southernmost record of the genus. The NW Pacific is inhabited by two newly described species: *O. lesci* and *O. claudei*, while in the eastern Pacific three species have been found so far: *O. denticulata, O. henrici* and *O. teresae.* A typical description of deep-sea fauna includes its rarity and patchy distribution (Kaiser *et al.*, 2007). Many of the species described from the deep sea have never been sampled anywhere else and are known only from the original type localities, often based on single individuals. According to the definitions used in Kaiser *et al.* (2007), all species of the genus *Oedicerina*,

apart from *O. ingolfi* and *O. lesci*, may be treated as rare taxa, whereas the cited two show patchiness of distribution (in the case of these species, > 75% of all known individuals were collected at two stations).

The analysis of bathymetric ranges of species within *Oedicerina* indicates two species inhabiting the upper bathyal (200–530 m), two species preferably occurring at middle and deep bathyal depths (1802–3200 m), and four species that are typical of the abyss (4050–5419 m) (Table 4). *O. claudei* was recorded at 3307 m in the Sea of Okhotsk, which at depths > 3000 m, is defined as an abyssal plain (Brandt *et al.*, 2019). At the time of this publication, the deepest record of the genus was 4050 m observed for *O. denticulata* in the north-east Pacific (Hendrycks & Conlan, 2003). Three out of four species presented here were collected in even deeper waters, with the deepest station at *c.* 5420 m, where this genus was observed in the abyss adjacent to the KKT.

ACKNOWLEDGEMENTS

The authors thank the chief scientists, scientific teams and crew of the expeditions during which the material was collected. The ABYSSLINE cruise was funded by UK Seabed Resources Ltd. The MANGAN 2016 and MANGAN 2018 cruises were funded by the BGR (Bundesanstalt für Geowissenschaften und Rohstoffe - German Federal Institute for Geosciences and Natural Resources). The SokhoBio expedition was organized with financial support from the Russian Science Foundation (Project No. 14-50-00034 to Dr. Marina V. Malyutina, Zhirmunsky National Scientific Center of Marine Biology, Far Eastern Branch, Russian Academy of Science). Material sorting was conducted with the financial support from the Bundesministerium für Bildung und Forschung - (BMBF German Ministry for Science and Education), grant 03G0857A to Prof. Dr. Angelika Brandt, University of Hamburg (current address Senckenberg Museum, Frankfurt, Germany). Both KuramBio I and II projects were supported by the Projektträger Jülich grants: KuramBio I BMBF, grant 03G0223A; KuramBio II BMBF, grant 03G0250A to Prof. Dr Angelika Brandt. The material of *O. ingolfi* from the North Atlantic was collected during the IceAGE1 expedition supported by the German Science Foundation (DFG, Deutsche Forschungsgemeinschaft) grant (BR3843/4-1) to Dr Saskia Brix, Senckenberg am Meer, German Centre for Marine Biodiversity Research (DZMB), Hamburg, Germany.

We would like to extend a special thank you to Dr Terue Cristina Kihara (Ines Solutions, Germany) for help during CLSM photograph preparations and to MSc. Katarzyna Kapuścińska (University of Lodz) who provided technical help for some of the laboratory work. Thanks are also due to the two anonymous reviewers whose work allowed us to greatly improve our manuscript and to Ms Joanna Leszczyńska for polishing the language of the text.

The molecular study of the material from the NW Pacific was conducted with support of a Polish National Science Centre grant (project no. 2014/15/D/NZ8/00289) to A.M.J. A.M.J. received financial support to visit Deutsches Zentrum für Marine Biodiversitätsforschung -(DZMB) in Wilhelmshaven (to study the collection of Pacific amphipods) from the German Academic Exchange Service (Deutscher Akademischer Austauschdienst -[DAAD]) within the program "Research Stays for University Academics and Scientists, 2019" (57440915). This is publication 71 of the Senckenberg am Meer Metabarcoding and DNA Laboratory. This is publication number 58 based on data from the Senckenberg am Meer Confocal Laser scanning Microscope Facility.

REFERENCES

Astrin JJ, **Stüben PE. 2008.** Phylogeny in cryptic weevils: molecules, morphology and new genera of western Palaearctic Cryptorhynchinae (Coleoptera: Curculionidae). *Invertebrate Systematics* **22:** 503–522.

Bandelt HJ, **Forster P**, **Röhl A. 1999.** Median-joining networks for inferring intraspecific phylogenies. *Molecular Biology and Evolution* **16:** 37–48.

Bober J, **Brandt A**, **Frutos I**, **Schwentner M. 2019.** Diversity and distribution of Ischnomesidae (Crustacea: Isopoda: Asellota) along the Kuril-Kamchatka Trench—a genetic perspective. *Progress in Oceanography* **178:** 102174.

Bober S, **Brix S**, **Riehl T**, **Schwentner M**, **Brandt A. 2018a.** Does the Mid-Atlantic Ridge affect the distribution of abyssal benthic crustaceans across the Atlantic Ocean? *Deep-Sea Research Part II* **148:** 91–104.

Bober S, **Riehl T**, **Henne S**, **Brandt A. 2018b.** New Macrostylidae (Isopoda) from the northwest Pacific Basin described by means of integrative taxonomy with reference to geographical barriers in the abyss. *Zoological Journal of the Linnean Society* **182:** 549–603.

Bonifácio P, **Menot L. 2019.** New genera and species from the Equatorial Pacific provide phylogenetic insights into deep-sea Polynoidae (Annelida). *Zoological Journal of the Linnean Society* **185:** 555–635.

Brandt A, **Alalykina I**, **Brix S**, **Brenke N**, **Błażewicz M**, **Golovan OA**, **Johannsen N**, **Hrinko AM**, **Jażdżewska AM**, **Jeskulke K**, **Kamenev GM**, **Lavrenteva AV**, **Malyutina MV**, **Riehl T**, **Lins L**, **2019.** Depth zonation of deep-sea macrofauna of the northwest Pacific. *Progress in Oceanography* **176:** 102131.

Brandt A, **Barthel D. 1995.** An improved supra- and epibenthic sledge for catching Peracarida (Crustacea, Malacostraca). *Ophelia* **43:** 15–23.

Brandt A, **Brix S**, **Riehl T**, **Malyutina M. 2020.** Biodiversity and biogeography of the abyssal and hadal Kuril-Kamchatka trench and adjacent NW Pacific deep-sea regions. *Progress in Oceanography* **181:** 102232.

Brandt A, **Elsner N**, **Brenke N**, **Golovan O**, **Malyutina MV**, **Riehl T**, **Schwabe E**, **Würzberg L. 2013.** Epifauna of the Sea of Japan collected via a new epibenthic sledge equipped with camera and environmental sensor systems. *Deep-Sea Research Part II* **86–87:** 43–55.

Brandt A, **Havermans C**, **Janussen D**, **Jörger KM**, **Meyer-Löbbecke A**, **Schnurr S**, **Schüller M**, **Schwabe E**, **Würzberg L**, **Zinkann A-C. 2014.** Composition of epibenthic sledge catches in the South Polar Front of the Atlantic. *Deep-Sea Research Part II* **108:** 69–75.

Brandt A, Malyutina MV, eds. 2015. The German-Russian deep-sea expedition KuramBio (Kurile Kamchatka Biodiversity Studies) to the abyssal area of the Kuril-Kamchatka Trench on board of the RV *Sonne* in 2012 following the footsteps of the legendary expeditions with RV *Vityaz*. *Deep-Sea Research Part II* **111:** 1–405.

Brenke N. 2005. An epibenthic sledge for operations on marine soft bottom and bedrock. *Marine Technology Society Journal* **39:** 10–21.

Britz R, **Hundsdörfer A**, **Fritz U. 2020.** Funding, training, permits—the three big challenges of taxonomy. *Megataxa* **1:** 49–52.

Brix S, **Bober S**, **Tschesche C**, **Kihara TC**, **Driskell A**, **Jennings RM. 2018a.** Molecular species delimitation and its implications for species descriptions using desmosomatid and nannoniscid isopods from the VEMA fracture zone as example taxa. *Deep-Sea Research Part II* **148:** 180–207.

Brix S, **Leese F**, **Riehl T**, **Kihara TC. 2015.** A new genus and new species of Desmosomatidae Sars, 1897 (Isopoda) from the eastern South Atlantic abyss described by means of integrative taxonomy. *Marine Biodiversity* **45:** 7–61.

Brix S, **Lörz A-N**, **Jażdżewska A**, **Hughes L**, **Tandberg AH**, **Pabis K**, **Stransky B**, **Krapp-Schickel T**, **Sorbe J-C**, **Hendrycks E**, **Vader WJM**, **Frutos I**, **Horton T**, **Jażdżewski K**, **Peart R**, **Beermann J**, **Coleman CO**, **Buhl-Mortensen L**, **Corbari L**, **Havermans C**, **Tato R**, **Jimenez Campean A. 2018b.** Amphipod family distributions around Iceland. *Zookeys* **731:** 41–53.

Brix S, **Osborn KJ**, **Kaiser S**, **Truskey SB**, **Schnurr SM**, **Brenke N**, **Malyutina M**, **Martinez Arbizu P. 2020.** Adult life strategy affects distribution patterns in abyssal isopods—implications for conservation in Pacific nodule areas. *Biogeosciences* **17:** 6163–6184.

Brix S, **Riehl T**, **Leese F. 2011.** First genetic data for species of the genus *Haploniscus* Richardson, 1908 (Isopoda: Asellota: Haploniscidae) from neighbouring deep-sea basins in the South Atlantic. *Zootaxa* **84:** 79–84.

Christodoulou M, **O'Hara T**, **Hugall AF**, **Khodami S**, **Rodrigues CF**, **Hilario A**, **Vink A**, **Martínez Arbizu P. 2020.** Unexpected high abyssal ophiuroid diversity in polymetallic nodule fields of the northeast Pacific Ocean, and implications for conservation. *Biogeosciences* **17:** 1845–1876.

Coleman CO. 2003. "Digital inking": how to make perfect line drawings on computers. *Organism, Diversity and Evolution, Electronic Supplement* **14:** 1–14.

Coleman CO. 2009. Drawing setae the digital way. *Zoosystematics and Evolution* **85:** 305–310.

Coleman CO, **Thurston MH. 2014.** A redescription of the type species of *Oedicerina* Stephensen, 1931 (Crustacea, Amphipoda, Oedicerotidae) and the description of two new species. *Zoosystematics and Evolution* **90:** 225–247.

d'Udekem d'Acoz C. 2004. The genus *Bathyporeia* Lindström, 1855, in western Europe: (Crustacea: Amphipoda: Pontoporeiidae). *Zoologische Verhandelingen Leiden* **348:** 3–162.

De Broyer C, **Chapelle G**, **Duchesne PA**, **Munn R**, **Nyssen F**, **Scailteur Y**, **Van Roozendael F**, **Dauby P. 2003.** Structural and ecofunctional biodiversity of the amphipod crustacean benthic taxocenoses in the Southern Ocean. In: *Marine biota and global change*, Belgian Scientific Research Programme on the Antarctic, Scientific results, Belgian Federal Public Planning Service Science Policy, Brussels, Belgium 58.

Delić T, **Trontelj P**, **Rendoš M**, **Fišer C. 2017.** The importance of naming cryptic species and the conservation of endemic subterranean amphipods. *Scientific Reports* **7:** 1–12.

Dong D, **Gan Z**, **Li X. 2021.** Descriptions of eleven new species of squat lobsters (Crustacea: Anomura) from seamounts around the Yap and Mariana Trenches with notes on DNA barcodes and phylogeny. *Zoological Journal of the Linnean Society*: zlab003. doi:10.1093/zoolinnean/zlab003.

Dreutter S, **Steffen M**, **Martínez Arbizu P**, **Brandt A. 2020.** Will the "top five" deepest trenches lose one of their members? *Progress in Oceanography* **181:** 102258.

Dupérré N. 2020. Old and new challenges in taxonomy: what are taxonomists up against? *Megataxa* **1:** 59–62.

Etter RJ, **Boyle EE**, **Glazier A**, **Jennings RM**, **Dutra E**, **Chase MR. 2011.** Phylogeography of a pan-Atlantic abyssal protobranch bivalve: implications for evolution in the Deep Atlantic. *Molecular Ecology* **20:** 829–843.

Felsenstein J. 1985. Phylogenies and the comparative method. *American Naturalist* **125:** 1–15.

Frutos I, **Brandt A**, **Sorbe JC. 2017.** Deep-sea suprabenthic communities: the forgotten biodiversity. In: Rossi S, Bramanti L, Gori A, Orejas C, eds. *Marine animal forests.* Cham: Springer International Publishing, 475–503.

Glover AG, **Dahlgren TG**, **Wiklund H**, **Mohrbeck I**, **Smith CR. 2016.** An end-to-end DNA taxonomy methodology for benthic biodiversity survey in the Clarion-Clipperton Zone, central Pacific abyss. *Journal of Marine Science and Engineering* **4:** 2.

Glover AG, **Smith CR**, **Paterson GLJ**, **Wilson GDF**, **Hawkins L**, **Sheader M. 2002.** Polychaete species diversity in the Central Pacific abyss: local and regional patterns, and relationships with productivity. *Marine Ecology Progress Series* **240:** 157–170.

Golovan OA, **Błażewicz M**, **Brandt A**, **Jażdżewska A**, **Jóźwiak P**, **Lavrenteva AV**, **Malyutina MV**, **Petryashov VV**, **Riehl T**, **Sattarova VV. 2019.** Diversity and distribution of peracarid crustaceans (Malacostraca)

from the abyss adjacent to the Kuril-Kamchatka Trench. *Marine Biodiversity* **49:** 1343–1360.

Hendrycks EA, **Conlan KE. 2003.** New and unusual abyssal gammaridean Amphipoda from the north-east Pacific. *Journal of Natural History* **37:** 2303–2368.

Horton T, **Lowry J**, **De Broyer C**, **Bellan-Santini D**, **Coleman CO**, **Corbari L**, **Costello MJ**, **Daneliya M**, **Dauvin J-C**, **Fišer C**, **Gasca R**, **Grabowski M**, **Guerra-García JM**, **Hendrycks E**, **Hughes L**, **Jaume D**, **Jazdzewski K**, **Kim Y-H**, **King R**, **Krapp-Schickel T**, **LeCroy S**, **Lörz A-N**, **Mamos T**, **Senna AR**, **Serejo C**, **Sket B**, **Souza-Filho JF**, **Tandberg AH**, **Thomas J**, **Thurston M**, **Vader W**, **Väinölä R**, **Vonk R**, **White K**, **Zeidler W. 2020.** *World Amphipoda Database*. Accessed at: http://www.marinespecies.org/amphipoda on 2020-04-04

Hou Z, **Fu J**, **Li S. 2007.** A molecular phylogeny of the genus *Gammarus* (Crustacea: Amphipoda) based on mitochondrial and nuclear gene sequences. *Molecular Phylogenetics and Evolution* **45:** 596–611.

Janssen A, **Kaiser S**, **Meißner K**, **Brenke N**, **Menot L**, **Martínez Arbizu P. 2015.** A reverse taxonomic approach to assess macrofaunal distribution patterns in abyssal Pacific polymetallic nodule fields. *PLoS One* **10:** 1–26.

Janssen A, **Stuckas H**, **Vink A**, **Martínez Arbizu P. 2019.** Biogeography and population structure of predominant macrofaunal taxa (Annelida and Isopoda) in abyssal polymetallic nodule fields: implications for conservation and management. *Marine Biodiversity* **49:** 2641–2658.

Jażdżewska A. 2015. Kuril-Kamchatka deep sea revisited—insights into the amphipod abyssal fauna. *Deep-Sea Research Part II* **111:** 294–300.

Jażdżewska AM, **Corbari L**, **Driskell A**, **Frutos I**, **Havermans C**, **Hendrycks E**, **Hughes L**, **Lörz A-N**, **Stransky B**, **Tandberg AHS**, **Vader W**, **Brix S. 2018.** A genetic fingerprint of Amphipoda from Icelandic waters—the baseline for further biodiversity and biogeography studies. *Zookeys* **731:** 55–73.

Jażdżewska AM, **Mamos T. 2019.** High species richness of northwest Pacific deep-sea amphipods revealed through DNA barcoding. *Progress in Oceanography* **178:** 102184.

Johannsen N, **Lins L**, **Riehl T**, **Brandt A. 2019.** Changes in species composition of Haploniscidae (Crustacea: Isopoda) across potential barriers to dispersal in the northwest Pacific. *Progress in Oceanography* **180:** 102233

Kaiser S, **Barnes DK**, **Brandt A. 2007.** Slope and deep-sea abundance across scales: Southern Ocean isopods show how complex the deep sea can be. *Deep-Sea Research Part II* **54:** 1776–1789.

Kaiser S, **Kihara TC**, **Brix S**, **Mohrbeck I**, **Janssen A**, **Jennings RM. 2021.** Species boundaries and phylogeographic patterns in new species of *Nannoniscus* (Janiroidea: Nannoniscidae) from the equatorial Pacific nodule province inferred from mtDNA and morphology. *Zoological Journal of the Linnean Society*: zlaa174. doi:10.1093/zoolinnean/zlaa174

Kamanli SA, **Kihara TC**, **Ball AD**, **Morritt D**, **Clark PF. 2017.** A 3D imaging and visualization workflow, using confocal microscopy and advanced image processing for brachyuran crab larvae. *Journal of Microscopy* **266:** 307–323.

Katoh K, **Misawa K**, **Kuma K**, **Miyata T. 2002.** MAFFT: a novel method for rapid multiple sequence alignment based on fast Fourier transform. *Nucleic Acids Research* **30:** 3059–3066.

Katoh K, **Standley DM. 2013.** MAFFT multiple sequence alignment software version 7: improvements in performance and usability. *Molecular Biology and Evolution* **30:** 772–780.

Khodami S, **Mercado-Salas NF**, **Martìnez Arbizu P. 2020.** Genus level molecular phylogeny of Aegisthidae Gisbrecht, 1893 (Copepoda: Harpacticoida) reveals morphological adaptations to deep-sea and plagic habitats. *BMC Evolutionary Biology* **20:** 36.

Kimura M. 1980. A simple method for estimating evolutionary rates of base substitutions through comparative studies of nucleotide sequences. *Journal of Molecular Evolution* **16:** 111–120.

Kumar S, **Stecher G**, **Tamura K. 2016.** MEGA7: molecular evolutionary genetics analysis version 7.0 for bigger datasets. *Molecular Biology and Evolution* **33:** 1870–1874.

Ledoyer M. 1986. Crustacés amphipodes gammariens. *Familles des Haustoriidae á Vitjazianidae. Faune de Madagascar 59(2).* Paris: ORSTOM Institut Français de Recherche Scientifique pour le Dévelopement en Coopération, 599–1112.

Lörz A-N, **Jażdżewska AM**, **Brandt A. 2018.** A new predator connecting the abyssal with the hadal in the Kuril-Kamchatka Trench, NW Pacific. *PeerJ* **6:** e4887.

Malyutina M, Brandt A, eds. 2013. SoJaBio (Sea of Japan biodiversity study). *Deep-Sea Research Part II* **86–87:** 1–238.

Malyutina MV, Chernyshev AV, Brandt A, eds. 2018. Introduction to the SokhoBio (Sea of Okhotsk biodiversity studies) expedition 2015. *Deep-Sea Research Part II* **154:** 1–382.

Michels J, **Büntzow M. 2010.** Assessment of Congo red as a fluorescence marker for the exoskeleton of small crustaceans and the cuticle of polychaetes. *Journal of Microscopy* **238:** 95–101.

Mitsuzawa K, **Holloway G. 1998.** Characteristics of deep currents along trenches in the northwest Pacific. *Journal of Geophysical Research: Oceans* **103:** 13085–13092.

Pleijel F, **Jondelius U**, **Norlinder E**, **Nygren A**, **Oxelman B**, **Schander C**, **Sundberg P**, **Thollesson M. 2008.** Phylogenies without roots? A plea for the use of vouchers in molecular phylogenetic studies. *Molecular Phylogenetics and Evolution* **48:** 369–371.

Ratnasingham S, **Hebert PD. 2007.** BOLD: the Barcode of Life Data System (http://www.barcodinglife.org). *Molecular Ecology Notes* **7:** 355–364.

Ratnasingham S, **Hebert PD. 2013.** A DNA-based registry for all animal species: the Barcode Index Number (BIN) System. *PLoS One* **8:** e66213.

Renz J, **Markhaseva EL**, **Laakmann S. 2019.** The phylogeny of Ryocalanoidea (Copepoda, Calanoida) based on morphology and a multi-gene analysis with a description of new ryocalanoidean species. *Zoological Journal of the Linnean Society* **185:** 925–957.

Riehl T, **Brenke N**, **Brix S**, **Driskell A**, **Kaiser S**, **Brandt A. 2014.** Field and laboratory methods for DNA studies on deep-sea isopod crustaceans. *Polish Polar Research* **35:** 203–224.

Riehl T, **Lins L**, **Brandt A. 2018.** The effects of depth, distance, and the Mid-Atlantic Ridge on genetic differentiation of abyssal and hadal isopods (Macrostylidae). *Deep-Sea Research Part II* **148:** 74–90.

Saeedi H, **Brandt A. 2020.** Introduction: biogeographic atlas of the deep NW Pacific fauna. In: Saeedi H, Brandt A, eds. *Biogeographic atlas of the deep NW Pacific fauna*. Sofia: Pensoft, 9–22.

Saitou N, **Nei M. 1987.** The neighbor-joining method: a new method for reconstructing phylogenetic trees. *Molecular Biology and Evolution* **4:** 406–425.

Stephensen K. 1931. Crustacea Malacostraca VII (Amphipoda III). *The Danish Ingolf-Expedition* **3:** 179–290.

Vause BJ, **Morley SA**, **Fonseca VG**, **Jażdżewska A**, **Ashton GV**, **Barnes DKA**, **Giebner H**, **Clark MS**, **Peck LS. 2019.** Spatial and temporal dynamics of Antarctic shallow soft-bottom benthic communities: ecological drivers under climate change. *BMC Ecology* **19:** 27.

Weisshappel JBF, **Svavarsson J. 1998.** Benthic amphipods (Crustacea: Malacostraca) in Icelandic waters: diversity in relation to faunal patterns from shallow to intermediate deep Arctic and North Atlantic Oceans. *Marine Biology* **131:** 133–143.

Wiklund H, **Neal L**, **Glover AG**, **Drennan R**, **Rabone M**, **Dahlgren TG. 2019.** Abyssal fauna of polymetallic nodule exploration areas, eastern Clarion-Clipperton Zone, central Pacific Ocean: Annelida: Capitellidae, Opheliidae, Scalibregmatidae, and Travisiidae. *ZooKeys* **883:** 1–82.

Zardus JD, **Etter RJ**, **Chase MR**, **Rex MA**, **Boyle EE. 2006.** Bathymetric and geographic population structure in the pan-Atlantic deep-sea bivalve *Deminucula atacellana* (Schenck, 1939). *Molecular Ecology* **15:** 639–651.

SUPPORTING INFORMATION

Additional Supporting Information may be found in the online version of this article at the publisher's web-site:

Table S1. Data on the individuals studied.